
Article:
Wang, R, Colombera, L orcid.org/0000-0001-9116-1800 and Mountney, NP (2020) Palaeohydrological characteristics and palaeogeographic reconstructions of incised-valley-fill systems: Insights from the Namurian successions of the United Kingdom and Ireland. Sedimentology. ISSN 0037-0746

https://doi.org/10.1111/sed.12773

Palaeohydrological characteristics and palaeogeographic reconstructions of incised-valley-fill systems: insights from the Namurian successions of the United Kingdom and Ireland

Ru Wang[1], Luca Colombera[1], and Nigel P. Mountney[1]

[1] Fluvial & Eolian Research Group and Shallow-Marine Research Group, School of Earth & Environment, University of Leeds, Leeds, LS2 9JT, UK

ABSTRACT

Namurian (Carboniferous) eustatic fluctuations drove the incision and backfill of shelf-crossing valley systems located in humid subequatorial regions, and now preserved in successions of the United Kingdom and Ireland. The infills of these valleys archive the record of palaeoriver systems whose environmental, hydrological and palaeogeographic characteristics remain unclear. A synthesis of sedimentological data from fluvial strata of 18 Namurian incised-valley fills (IVFs) in the United Kingdom and Ireland is undertaken to elucidate the nature of their formative river systems and to refine regional palaeogeographic reconstructions. Quantitative analyses are performed of facies proportions, of geometries of IVFs and related architectural elements, and of the thickness of dune-scale sets of cross-strata. Reconstruction of the size of the drainage areas that fed these valleys is attempted based on two integrative approaches: flow-depth estimations from dune-scale cross-set thickness statistics and scaling relationships of IVF dimensions derived from late-Quaternary IVFs.

The facies organization of these IVFs suggests that their formative palaeorivers were perennial and experienced generally low discharge variability, consistent with their climatic context; however, observations of characteristically low variability in cross-set thickness might reflect rapid flood recession, perhaps in relation to sub-catchments experiencing seasonal rainfall. Variations in facies characteristics, including inferences of flow regime and cross-set thickness distributions, might reflect the control of catchment size on river hydrology, the degree to which is considered in light of data from modern rivers. Palaeohydrological reconstructions indicate that depth estimations from cross-set thickness contrast with observations of barform and channel-fill thickness, and projected thalweg depths exceed the depth of some valley fills. Limitations in data and interpretations and high bedform preservation are recognized as possible causes. With consideration of uncertainties in the inference of catchment size, the palaeogeography of the valley systems has been tentatively reconstructed by integrating existing provenance and sedimentological data.

The approaches illustrated in this work can be replicated to the study of palaeohydrologic characteristics and palaeogeographic reconstructions of incised-valley fills globally and through geological time.

Keywords: incised valley, drainage basin, fluvial, palaeohydrology, palaeogeography, sea-level change

INTRODUCTION

Valleys produced by river incision are topographic lows that are larger than their formative rivers, which are typically unable to flood beyond the valley walls and onto the interfluves (Gibling et al., 2011; Holbrook and Bhattacharya, 2012). Nearshore incised valleys develop in coastal-plain to continental-shelf regions in response to relative sea-level fall, and tend to be subsequently inundated, infilled and reworked by fluvial, coastal and marine processes during relative sea-level rise (Posamentier and Allen, 1999; Zaitlin et al, 1994; Blum et al., 2013). Extensive research has been undertaken on both recent and ancient nearshore incised-valley-fill successions because of their potential to archive complex sedimentary responses to relative changes in sea level and climate (Boyd et al., 2006; Simms et al., 2010; Mattheus and Rodriguez, 2011), and because of their importance as hosts for natural resources, notably as hydrocarbon reservoirs (Hampson et al., 1999; Stephen and Dalrymple, 2002; Bowen and Weimer, 2003; Salem et al., 2005).

Quaternary incised-valley fills arising as a consequence of icehouse glacio-eustatic cyclicity record incision and infill by trunk rivers that traversed coastal plains extending to continental-shelf margins. The rivers that generated these valleys commonly merged on lowstand shelves, such that their drainage basins amalgamated into alluvial catchments that were larger than the modern highstand drainage basins composing their fragments (e.g., Wong et al., 2003; Anderson et al., 2004; Maselli et al., 2014; Collier et al., 2015; Alqahtani et al., 2015; cf. Blum and Womack, 2009; Blum et al., 2013). In the rock record, sedimentary bodies interpreted as incised-valley fills developed primarily under icehouse conditions contain sedimentological evidence of the scale of many large river systems that existed throughout Earth history, and can therefore provide insight into palaeogeographic configurations.

In the Namurian – a regional stage of the Carboniferous (late Mississippian [Serpukhovian] to early Pennsylvanian [Bashkirian]) used in Western Europe – thick sandstone-dominated fluvial deposits have been well documented in outcropping and subsurface successions of the United Kingdom (UK) and Ireland. These fluvial deposits are interpreted to form the majority of the infill of cross-shelf incised valleys. These incised-valley-fill (IVF) successions are interpreted to have developed in response to high-frequency, high-magnitude eustatic sea-level changes in relation to Gondwanan glacial-interglacial episodes (Hampson et al., 1997; Hampson et al., 1999; Davies et al., 1999; Davies, 2008). During the Namurian, a suite of sedimentary basins in the region now occupied by the UK and Ireland existed that was part of a series of linked basins that extended across what is now NW Europe and eastern Canada. The sedimentary infill of these basins occurred at palaeoequatorial latitudes (**Fig. 1**), under conditions of overall humid tropical climate (Davies et al., 1999; Davies, 2008; Boucot et al., 2013). Fifty Namurian, ammonoid-bearing (goniatite) marine bands are identified in these successions (**Fig. 2**). These thin marine beds of fossiliferous carbonaceous mudstones bearing diagnostic thick-shelled ammonoids are widespread, and many of them can be correlated confidently in successions across northwest Europe (Davies et al., 1999; Waters and Condon, 2012), providing exceptionally high biostratigraphic resolution for the studied areas (Davies et al., 1999; Davies, 2008; Waters and Condon, 2012). Previous work in Namurian basins of the UK and Ireland (e.g., Bristow and Myers, 1989; Bristow, 1993; Hampson et al., 1999; Ellen et al., 2019) has focused on qualitative analyses of the internal facies architecture of these IVFs, which led these workers to interpret the river systems feeding these IVFs as having low-sinuosity, probably braided, planforms at low-river stage. Provenance studies (e.g., Hallsworth et al., 2000; George, 2001;

Hallsworth and Chisholm, 2008; Pointon et al., 2012) are also available for these IVFs, which provide insights regarding the likely source areas and extent of their formative rivers. However, questions still remain in relation to the palaeohydrology and palaeogeography of these river systems, and such questions can potentially be answered with additional analyses of sedimentological and architectural characteristics of the several examples of IVFs identified in these successions.

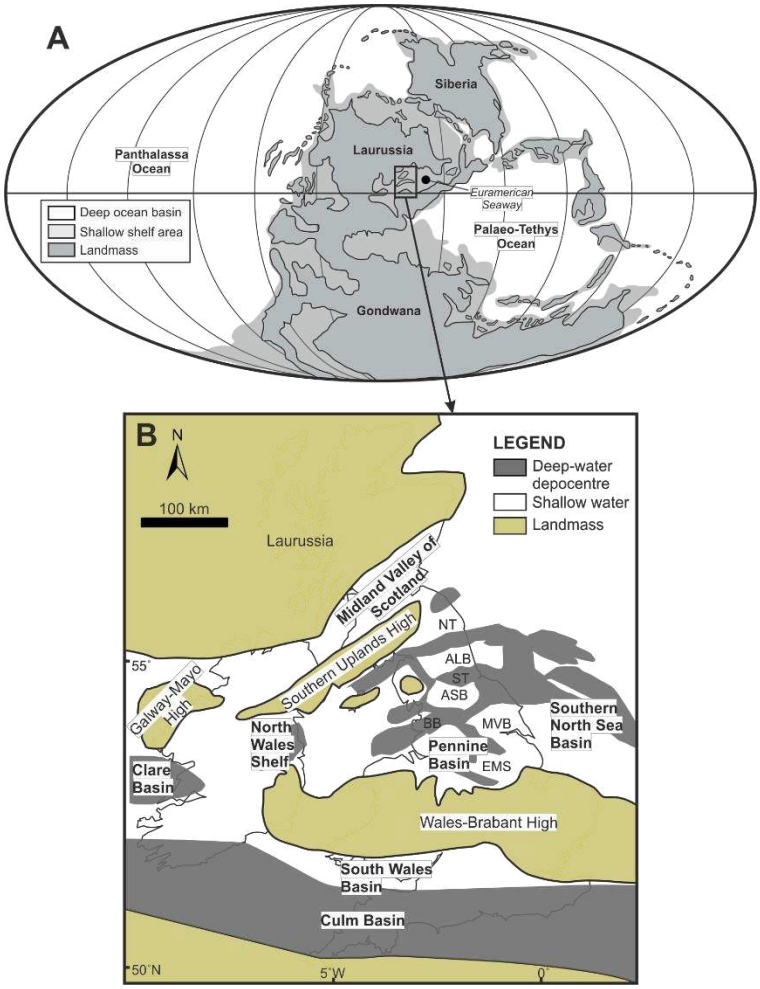

Fig. 1. (A) Global palaeogeographic map for the late Mississippian, with inset map (B) illustrating landmasses, deep-water depocentres and shallow-water areas across the UK and Ireland during the late Mississippian. Note that the extent of Gondwanan ice sheets is not shown in (A). Modified from Davies et al. (2012) and Davies (2008). Selected palaeogeographic and basin names discussed in this paper are shown. ALB = Alston Block; ASB = Askrigg Block; BB = Bowland Basin; EMS = East Midlands Shelf; MVB = Market Weighton Block; ST = Stainmore Trough; NT = Northumberland Trough.

In this study, a database-driven synthesis of data from 18 Namurian incised-valley fills from the UK and Ireland has been performed to quantitatively estimate palaeohydrological characteristics of these ancient river systems, and to attempt to refine the regional palaeogeographic reconstructions for the basins that hosted them. Specific objectives of this work are as follows: (i) to decipher palaeohydraulic characteristics from facies proportions and geometry of cross-strata within incised-valley fluvial deposits; (ii) to investigate upstream controls on the facies architecture of incised-valley fluvial deposits; (iii) to illustrate a novel integrated approach to the estimation of the size of drainage areas for deep-time incised-valley fills, based on dune-scale cross-set thickness and incised-valley-fill dimension; (iv) to present how results have implications for regional palaeogeographic reconstructions, when considered in combination with provenance studies and other sedimentological data.

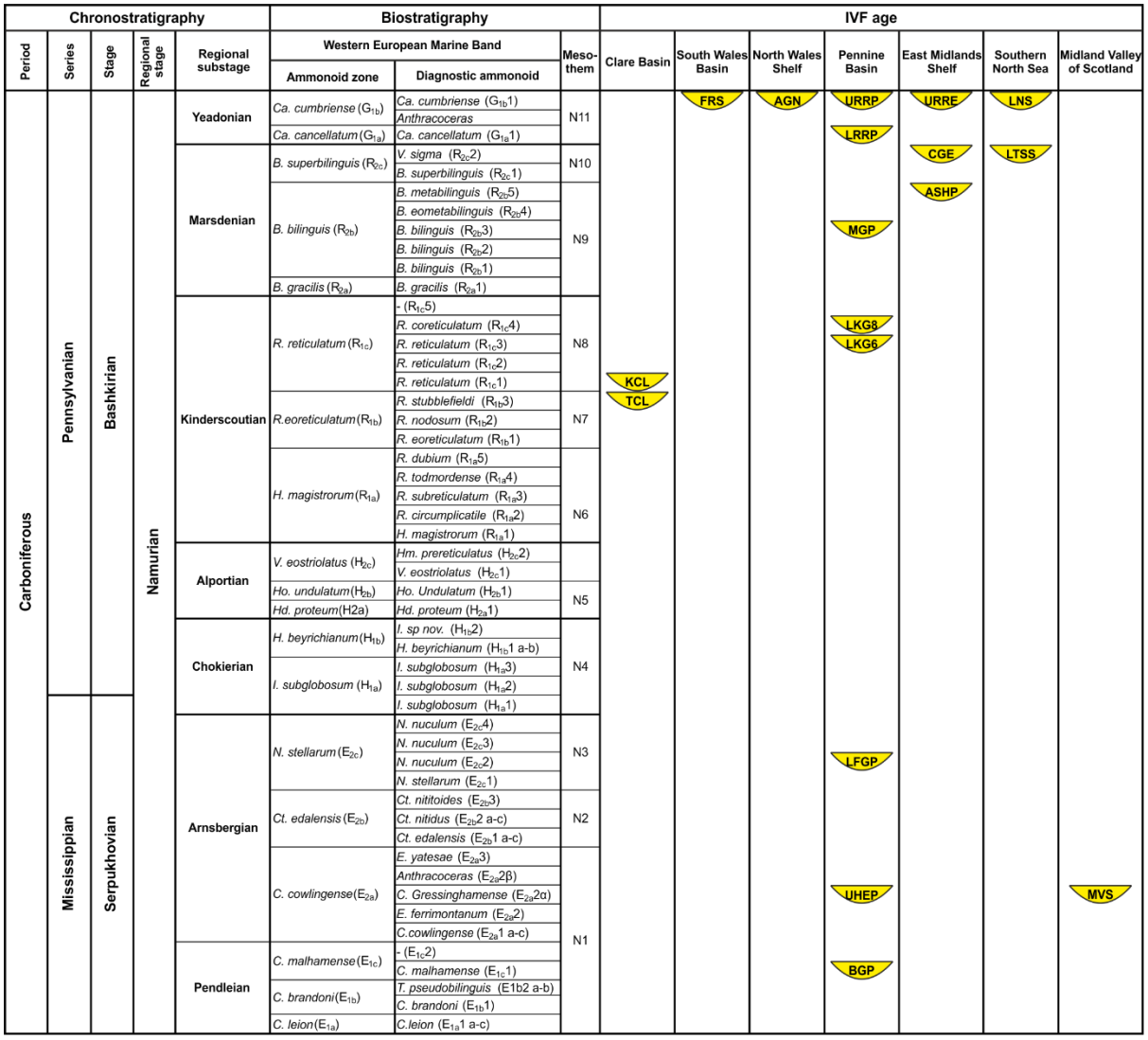

Fig. 2. Schematic stratigraphic columns for selected Namurian basins in the UK and Ireland, illustrating the age of the studied incised-valley fills (IVFs) considered in this work. Modified from Dean et al. (2011), Waters and Condon (2012) and Bijkerk (2014). Abbreviations for ammonoid taxa: B = *Bilinguites*; Ca = *Cancelloceras*; C = *Cravenoceras*; Ct = *Cravenoceratoides*; E = *Eumorphoceras*; H = *Hodsonites*; Hd = *Hudsonoceras*; Hm = *Homoceratoides*; Ho = *Homoceras*; I = *Isohomoceras*; N = *Nuculoceras*; R = *Reticuloceras*; V= *Verneulites*.

GEOLOGICAL SETTING

In the UK and Ireland, basin evolution during the early Carboniferous between the Wales-Brabant High and Southern Uplands High was strongly influenced by the reactivation of late Caledonian basement structures, resulting in the development of a series of fault-controlled extensional basins and structurally emergent blocks (Gawthorpe et al., 1989; Chadwick et al., 1995; Kirby et al., 2000**; Fig. 1**). During the Namurian, active rifting became less important and regional thermal subsidence was dominant in this region (Waters and Davies, 2006; Davies, 2008; Davies et al., 2012). To the south of the Wales-Brabant High, the South Wales Basin was affected by the Variscan orogeny (Dunne et al., 1980; Dunne, 1983; Hancock and Tringham, 1983; Smallwood, 1985; Powell, 1987, 1989) and formed one of several E-W-trending foreland basins (George, 2001; Davies, 2008). The late-Namurian strata relating to the deposition of the Farewell Rock IVF studied in this work were deposited on the cratonic margin of the foredeep zone of this foreland basin (George, 2001).

During the late Mississippian to early Pennsylvanian (Namurian), the studied basins were located at near-equatorial palaeolatitudes, a few degrees north of the equator (**Fig. 1**; Scotese and McKerrow, 1990; Douwe et al., 2015; Blakey, 2016). Palaeoclimatic evidence exists for these successions in the form of palaeosols (gleysols; Davies, 2008; Davies et al., 2012), palynology (Van der Zwan et al., 1985), the presence of widespread coals (Davies, 2008; Davies et al., 2012; Boucot et al., 2013), and weathering products (bauxites, kaolinite in latosols; Witzke, 1990; Boucot et al., 2013), indicating that the prevailing climates were characterized by predominantly humid tropical conditions and short-term seasonally drier intervals (Davies, 2008; Davies et al., 2012; Boucot et al., 2013).

The different Namurian basins of the UK and Ireland all display similar infill motifs (Collinson, 1988). The earliest stage of basin fill led to accumulation of mudstones of deep-water origin, which tended to be deposited in the basin depocentres. Overlying deposits typically comprise a turbidite-fronted deltaic succession, which tended to infill the inherited bathymetry of a particular basin or sub-basin. After the inherited bathymetry was infilled, the basin was subsequently filled by a widespread shallow-water deltaic succession. Many thick sandstone-dominated fluvial deposits occurred within turbidite-fronted deltaic or shallow-water deltaic successions and were interpreted as valley fills that cut into marine or coastal deposits during episodes of falling sea level (Hampson et al., 1997; Hampson et al., 1999; Davies et al., 1999; Davies, 2008). These units are the focus of this work.

Global sea-level fluctuations during the Namurian were characterized by high-frequency and high-magnitude sea-level changes, due to the waxing and waning of Gondwanan ice sheets (Maynard and Leeder, 1992; Hampson et al., 1997; Wright and Vanstone, 2001). Fifty continental-scale ammonoid-bearing marine bands, interpreted as marking the position of maximum flooding surfaces relating to glacio-eustatic sea-level rises (e.g., Maynard, 1992; Church and Gawthorpe, 1994; Martinsen et al., 1995; Hampson et al., 1997; Davies et al., 1999), are identified in Namurian siliciclastic successions in the UK and Ireland (Waters and Condon, 2012; **Fig. 2**). Regional unconformities forming the bases of the incised valleys correspond to the 'master' sequence boundaries (*sensu* Posamentier and Allen, 1999; e.g., Martinsen et al., 1995; Hampson et al., 1997; Davies et al., 1999; Brettle, 2001) and approximately fifty 'master' sequences (lower-order sequences *sensu* Posamentier and Allen, 1999) are identified in the studied 'Namurian' succession (Hampson et al., 1997; Davies et al., 1999; Davies, 2008; Waters and Condon, 2012). According to different authors, the mean periodicity of the marine bands has been estimated at 185 kyr (Holdsworth and Collinson, 1988; Martinsen et al., 1995), 120 kyr (Maynard and Leeder, 1992), 90 kyr (Collinson, 2005) or 65 kyr based on SHRIMP U–Pb zircon dating (Riley et al., 1995). These values are consistent with fourth-order cyclicity *sensu* Mitchum and Van Wagoner (1991). According to different authors, the magnitude of eustatic sea-level fluctuations has been estimated at ca. 42 m (Maynard and Leeder, 1992), 60 m (Church and Gawthorpe, 1994) or 65 ± 15 m (Crowley and Baum, 1991). Based on the depth of incision of palaeovalleys, Rygel et al. (2008) reported glacio-eustatic sea-level oscillations of 60-100 m during the Namurian. Magnitudes and periodicities of eustatic sea-level modulation during the Namurian were similar to those of Late Quaternary glacial-interglacial cycles (Brettle, 2001).

METHODOLOGY

Database

A synthesis of data from 18 interpreted incised-valley fills (IVFs) from Namurian successions of the UK and Ireland is undertaken here. Data on the sedimentology of fluvial

deposits forming part of these IVFs are included in a relational database, the Fluvial Architecture Knowledge Transfer System (FAKTS; Colombera et al., 2012). FAKTS stores data on the geometry, spatial relationships, and hierarchical relationships of genetic units such as 'depositional elements', 'architectural elements' and 'facies units'; these genetic units are assigned to subsets of fluvial systems, themselves classified on multiple parameters (e.g., climate, tectonic setting, catchment area) and metadata (e.g., data quality, data types). Facies units in FAKTS represent lithofacies classified by grainsize and sedimentary structures, and are delimited by bounding surfaces that correspond to a change in lithofacies type or palaeocurrent direction, or to erosional contacts or element boundaries (Colombera et al., 2013).

The sedimentological data relating to the IVFs studied in this work have been derived from 27 literature sources and one original field study. A detailed account of the IVFs considered in this work, their corresponding published-source references, the types of the data available for each, and their geographic location is shown in **Table 1**; the age and stratigraphic occurrence of the studied IVFs is reported in **Fig. 2**. For the studied examples, investigations of the facies architecture of their fluvial deposits are generally based on outcrop exposures in South Wales, North Wales, northern England, Scotland and Northern Ireland, and on subsurface datasets from the East Midlands Shelf and the Southern North Sea (**Table 1**).

The scheme for the classification of facies units adopted in FAKTS (Colombera et al., 2013) is adapted and extended from the earlier scheme by Miall (1996); the facies types identified in the studied IVF fluvial deposits are reported in **Table 2**. The classifications of facies types in the database rely upon interpretations given in the original works. To facilitate analysis and to establish an audit trail, the detailed facies descriptions reported in the original sources are also recorded, but are not used in this work. The relative proportion of each facies type within IVF fluvial deposits has been calculated based on the sum of their measured thicknesses.

Dune-scale cross-set thickness

The thickness of cross-sets in dune-scale cross-stratification (planar and trough cross-stratification) has been measured directly on logged sections or outcrop panels using image-analysis software (ImageJ; Schneider et al., 2012) for the fluvial deposits of each IVF. Only dune-scale cross sets in sandstones and conglomerates are included in the dataset; sedimentary structures that are interpreted to represent preserved macroforms (bars, *sensu* Jackson, 1975; Bridge, 2003) or microforms (ripple cross-laminations; *sensu* Allen, 1982; Bartholdy et al., 2015) have not been considered. Isolated cross-sets that were originally interpreted to be formed by unit bars (Bridge and Tye, 2000) are also excluded. Cross-sets interpreted as the expression of smaller dunes superimposed on larger dunes are also not considered, since these bedforms might reflect local flow conditions over the larger host bedforms (Jackson, 1975; Soltan and Mountney, 2016). Suitable data on dune-scale cross-set thickness are available for 15 of the 18 valley fills; the three remaining examples (Ashover Grit, East Midlands Shelf; Bearing Grit, Pennine Basin; late Namurian valley fill from the southern North Sea Basin) are excluded because the cross sets represented in the original datasets are not depicted in their true scale.

Table 1. Namurian incised-valley fills of the UK and Ireland stored in the Fluvial Architecture Knowledge Transfer System (FAKTS) database and considered in this study. For each example, the table reports its

acronym as used in this work (column IVF), location, basin name, lithostratigraphic unit, published literature sources and data types. Fm. = Formation; Gp. = Group.

IVF	Location	Basin	Lithostratigraphic unit	Data source	Data type	Spatial type
MVS	Scotland	Midland Valley Basin	Spireslack Sandstone, Upper Limestone Fm.	Ellen et al. (2019)	Outcrops	2D section
TCL	Western Ireland	Shannon Basin (Clare Basin)	Tullig Sandstone	Stirling (2003); Best et al. (2016)	Outcrops	2D section
KCL	Western Ireland	Shannon Basin (Clare Basin)	Kilkee Sandstone	Pulham (1988)	Outcrops	2D section
AGN	North Wales	Pennine Basin (North Wales Shelf)	Aqueduct Grit, Gwespyr Sandstone	Jerrett and Hampson (2007)	Outcrops	2D section
LKG 6	England	Pennine Basin	Lower Kinderscout Grit, Millstone Grit Gp.	Hampson (1997)	Outcrops	1D vertical
LKG 8	England	Pennine Basin	Lower Kinderscout Grit, Millstone Grit Gp.	Hampson (1997)	Outcrops	1D vertical
LRRP	England	Pennine Basin	Lower Rough Rock, Millstone Grit Gp.	Hampson et al. (1996); Hampson (1995)	Outcrops	2D section
URRP	England	Pennine Basin	Upper Rough Rock, Millstone Grit Gp.	Hampson et al. (1996); Hampson (1995)	Outcrops	2D section
URRE	England	Pennine Basin (East Midlands Shelf)	Upper Rough Rock, Millstone Grit Gp.	Hampson et al. (1996); Church and Gawthorpe (1994); Hampson (1995)	Outcrops	2D section
ASHP	Southern England	Pennine Basin (East Midlands Shelf)	Ashover Grit, Millstone Grit Gp.	Church and Gawthorpe (1994); Jones and Chisholm (1997)	Cores	1D vertical
CGE	Southern England	Pennine Basin (East Midlands Shelf)	Chatsworth Grit, Millstone Grit Gp.	O'Beirne (1996); Waters et al. (2008)	Outcrops	2D section
MGP	Northern England	Pennine Basin	Midgley Grit, Millstone Grit Gp.	Brettle et al. (2002); Brettle (2001)	Outcrops	2D section
UHEP	Northern England	Pennine Basin	Upper Howgate Edge Grit, Millstone Grit Gp.	Martinsen (1993)	Outcrops	1D vertical
LFGP	Northern England	Pennine Basin	Lower Follifoot Grit, Millstone Grit Gp.	Martinsen et al. (1995); Martinsen (1990)	Outcrops	1D vertical
BGP	Northern England	Pennine Basin	Bearing Grit, Millstone Grit Gp.	Bijkerk (2014)	Outcrops	2D section
LNS	Southern North Sea	Southern North Sea Basin	Millstone Grit Gp.	George (2001)	Cores, Well logs	1D vertical
LTSS	Southern North Sea	Southern North Sea Basin	Lower Trent Sandstone, Millstone Grit Gp.	O'Mara et al. (1999)	Cores, Well logs	1D vertical
FRS	South Wales	South Wales Basin	Farewell Rock, Upper Sandstone Gp.	original field study; George (2001)	Outcrops	2D section

Table 2. Scheme adopted for the classification of lithofacies of fluvial deposits. The facies types are employed in FAKTS (Colombera et al., 2012, 2013), and are adapted and extended from those by Miall (1996).

Code	Characteristics
G-	Conglomerate with undefined structure and undefined additional textural characteristics.
Gmm	Matrix-supported, massive or crudely bedded conglomerate.
Gmg	Matrix-supported, graded conglomerate.
Gcm	Clast-supported, massive conglomerate.
Gci	Clast-supported, inversely graded conglomerate.
Gh	Clast-supported, horizontally or crudely bedded conglomerate; possibly imbricated.
Gt	Trough cross-stratified conglomerate.
Gp	Planar cross-stratified conglomerate.
S-	Sandstone with undefined structure.
St	Trough cross-stratified sandstone.
Sp	Planar cross-stratified sandstone.
Sr	Current ripple cross-laminated sandstone.
Sh	Horizontally bedded sandstone.
Sl	Low-angle (<15°) cross-bedded sandstone.
Ss	Faintly laminated, cross-bedded, massive or graded sandstone fill of a shallow scour.
Sm	Massive sandstone; possibly locally graded or faintly laminated.
Sd	Soft-sediment deformed sandstone.
F-	Fine-grained deposits (siltstone, claystone) with undefined structure.
Fl	Interlaminated very-fine sandstone, siltstone and claystone; might include thin cross-laminated sandstone lenses.
Fsm	Laminated to massive siltstone and claystone.
Fm	Massive claystone.
Fr	Fine-grained rooted bed.
C	Coal or highly carbonaceous mudstone.

Incised-valley-fill dimensions

IVF dimensions are derived from the original source work, either obtained from the primary text or measured directly on figures using image-analysis software (ImageJ; Schneider et al., 2012). The measurement of IVF dimensions follows the method by Wang et al. (2019). IVF thickness (T) is defined as the vertical distance between the elevation of the lowermost point of the erosional IVF base and the height of the interfluves at the valley margins. IVF width (W) is defined as the maximum horizontal distance between the valley walls as measured perpendicular to the valley axis. IVF dimensions are expected to vary along dip (Strong and Paola, 2008; Martin et al., 2011; Phillips, 2011). In this work, the largest observed values of valley-fill thickness and width along the valley reach are recorded. IVF thickness usually differs from the thickness of IVF fluvial deposits, for example because incised valleys are partly filled by estuarine deposits (e.g., Farewell Rock IVF in South Wales, Lower Trent Sandstone IVF in the southern North Sea). Based on the reported geometry of IVF fluvial sandstones, the IVF cross-sectional area is approximated by a half-elliptical or rectangular shape (respectively as $\pi/4 \times T \times W$ or $T \times W$, where T is IVF thickness and W is IVF width, both in metres). For instance, the IVF geometries for the lower and upper Rough Rock examples from the Pennine Basin and for the Upper Rough Rock example from the East Midlands Shelf (LRRP, URRP and URRE in **Table 1**) are originally described as sheet-like, and accordingly the corresponding IVF cross-sectional areas are approximated as rectangular.

Estimation of drainage-area size

To estimate the size of the drainage area upstream of the location where the studied IVF is characterized, two integrative approaches are employed in this work.

Estimation of drainage area from cross-set thickness

Scaling between cross-set thickness, dune height and formative flow depth

Previous theoretical, experimental (Bridge and Tye, 2000; Leclair and Bridge, 2001; Leclair, 2002; Jerolmack and Mohrig, 2005) and numerical studies (Leclair, 2002; Jerolmack and Mohrig, 2005; Ganti et al., 2013) have demonstrated that both the mean thickness (s_m) of a cross set, considered relative to the mean formative bedform height (h_m), and the coefficient of variation (ratio of standard deviation to mean) of the preserved cross-set thickness (CV (d_{st})) remain relatively constant ($s_m / h_m \approx 0.3$; CV (d_{st}) ≈ 0.88) under steady flow conditions and no net aggradation.

The following equation has been used to estimate the formative bedform height:

$h_m = 2.9(\pm 0.7)\ s_m$ (Leclair and Bridge, 2001; cf. Leclair et al., 1997; Bridge, 1997; Bridge and Tye, 2000)

This empirical equation is indicated to be only applicable when the coefficient of variation of cross-set thickness CV (d_{st}) equals to 0.88 ± 0.3 (Bridge and Tye, 2000). Ideally, when employing this method, it must be accepted (Bridge and Tye, 2000; cf. Leclair et al., 1997; Bridge, 1997) that: (1) the distribution of cross-set thickness primarily depends on variability in dune height; (2) variations in aggradation rate exert a limited control on set thickness (cf. Leclair et al., 1997; Bridge, 1997); (3) cosets of cross-strata are homogeneous in time and space, i.e., lack obvious temporal and spatial variations in cross-strata type or mean grain size; (4) angles of bedform climb are negligible (Paola and Borgman, 1991). Based on values returned by the experiments of Leclair et al. (1997), this CV (d_{st}) criterion is an initial test of the applicability of the empirical equation of Leclair and Bridge (2001).

A scaling relation derived from field observations by Bradley and Venditti (2017) has been used to estimate the formative flow depth (d), from estimated dune height (h) as:

$d = 6.7\ h$ (with 50% prediction interval: 4.4h-10.1h) (Bradley and Venditti, 2017)

In this work, these empirical equations have been utilized to estimate the mean bankfull depth for the formative rivers of the studied IVFs from mean dune height, themselves estimated from the mean value of measured cross-set thickness (cf. Bridge and Tye, 2000; Holbrook and Wanas, 2014; Buller et al., 2018; Ganti et al., 2019a).

Regional hydraulic-geometry curves for estimating drainage areas

For the prediction of drainage areas, Davidson and North (2009) recommend the use of regional hydraulic-geometry curves obtained from modern drainage-basin surveys, which relate mean bankfull depth to drainage area under differing climatic, physiographic and latitudinal conditions. Mean bankfull depth is defined as the mean depth of the bankfull channel measured perpendicular to streamflow and expressed by the ratio between bankfull cross-sectional area and bankfull width (USDA-NRCS-NWMC 2009). In this work, the approach of Davidson and North (2009) is employed to estimate the drainage areas from the estimated mean bankfull depth.

During the Namurian, the study areas were located a few degrees north of the palaeo-equator (Scotese and McKerrow, 1990; Blakey, 2016) and were characterized by

predominantly humid tropical conditions with short-term seasonally drier intervals (Davies, 2008; Davies et al., 2012; Boucot et al., 2013). The Pennine drainage system is interpreted to have derived sediments from Caledonian uplands, which were located to the north of the Pennine Basin, in an area corresponding to present-day Greenland and lying between ca. 10° and 20° latitude (Hallsworth et al., 2000). This implies that a part of the drainage basin might have been located in the seasonal tropics and is likely to have received variable, possibly monsoonal, precipitation throughout the year (Bijkerk, 2014). A regional curve that is ideally suited to the palaeoclimate or palaeolatitude of the Namurian basins of the UK and Ireland is not available among those presented by Davidson and North (2009), whose compilations relating to coastal-plain regions of north Florida, northwest Florida, North Carolina and Maryland (USA) can be considered as the most relevant for this study. The Amazon basin is likely to be a more appropriate analogue, since the Amazon catchment is located near the equator and is predominantly characterized by tropical rainforest climate, with subordinate tropical monsoon climate. A regional curve for rivers of the Amazon basin is compiled by Beighley and Gummadi (2011) using gauging station records and drainage-network reconstructions based on remotely sensed data (Lehner et al., 2008). Even though these modern analogues may not perfectly match the palaeoclimate or palaeolatitude of the studied Namurian basins, they allow an assessment of the likely range in size of drainage areas.

The approach proposed by Davidson and North (2009) is based on inversion of the direct relations between mean bankfull depth and drainage area to reconstruct drainage areas from mean bankfull depth, which can be estimated from observations from the rock record. However, to be able to present prediction intervals, corresponding relations have been recompiled based on the data reported in the original sources whereby mean bankfull depth and drainage area are independent and dependent variables respectively (**Fig. 3**). Unlike Davidson and North (2009), who quantified these two variables in imperial units, metric units are used here (**Fig. 3**). To present the uncertainty in the estimated size of drainage areas for the ancient rivers feeding the studied IVFs, 95% confidence and prediction intervals are constructed for relationships between the two variables (**Fig. 3**). 95% prediction intervals are utilized in the subsequent analyses to carry the sample variability forward as a form of uncertainty (cf. James et al., 2013).

For comparison with estimations obtained with other methods, a scaling relation between drainage area *versus* mean bankfull depth has also been derived for all the data from all the aforementioned modern analogues ('average modern analogue', hereafter). For simplicity, the resultant estimated drainage areas are also used in the subsequent analyses, for investigating the relationships between facies architecture within incised-valley fluvial deposits and the size of the drainage basins feeding their formative river systems.

Based on the reconstructed scaling relationships for individual modern analogues (**Fig. 3A-E**) and for their collective dataset (**Fig. 3F)**, drainage areas are estimated from reconstructions of mean bankfull depth, itself based on mean values of cross-set thickness, for the 15 IVFs for which dune-scale cross-set thickness data are available (see above).

Estimation of drainage area from incised-valley-fill dimensions

The dimensions of nearshore incised valleys are determined by a number of factors, including the magnitude and rate of relative base-level fall, contributing drainage-basin size, climate, basin physiography, substrate types and tectonics (Talling, 1998; Posamentier, 2001; Gibling 2006; Strong and Paola, 2006, 2008; Martin et al., 2011; Blum et al., 2013; Wang et al., 2019). Based on statistical analysis of global 'icehouse' late-Quaternary incised valleys,

previous workers (Mattheus et al., 2007; Mattheus and Rodriguez, 2011; Phillips, 2011; Wang et al., 2019) have demonstrated that, for a relative sea-level fall of a given magnitude, valley dimensions at comparable locations along their dip extent are strongly correlated with the drainage-basin area of their formative rivers, and that for passive margins, water discharge exerts a primary control on valley-fill shape and size. This is especially true for 'fast' cycles of relative sea-level change where lateral reworking and valley widening at lowstand is more limited compared to slower cycles with prolonged lowstands (Strong and Paola, 2008; Wang et al., 2009). Here, 'fast' is defined with respect to a theoretical equilibrium time, which characterizes the natural response time of a depositional basin to imposed change and is primarily determined by basin dimensions, sediment supply and water discharge (Paola et al., 1992). Considering the similarity in magnitude and frequency of eustatic sea-level changes during Namurian and late-Quaternary times, and given the relatively quiescent tectonic context of the Namurian basins of the UK and Ireland, the scaling relations developed from the late-Quaternary valleys (Wang et al., 2019) can be tentatively applied to the Namurian examples in this work. Accordingly, drainage areas of 10 incised valleys considered in this work have been estimated based on the approximated IVF cross-sectional area, utilizing the scaling relationship derived from late-Quaternary examples (Wang et al., 2019). A scaling relation between drainage area and IVF cross-sectional area for late-Quaternary IVFs from passive continental margins (**Fig. 4**) is derived on the basis of data from Wang et al. (2019). Ideally, IVF thickness should be used as predictor, since this is a parameter that is generally easier to constrain in the stratigraphic record. However, since the relationship between drainage area and IVF cross-sectional area for late-Quaternary IVFs is stronger than that between drainage area and IVF thickness or width (Wang et al., 2019), and considering that valley incision is more sensitive to basin physiography (Bijkerk, 2014; Wang et al., 2019), the IVF cross-sectional area is utilized in this work for prediction of valley drainage areas. However, IVF cross-sectional areas are estimated based on the extrapolation of local observations and not measured directly. Additionally, this approach carries uncertainties as the dimensions of incised-valley fills vary along their depositional dip (Strong and Paola, 2008; Martin et al., 2011; Phillips, 2011), and therefore the location and spatial extent of observations affect IVF dimensional parameters. In this work, for both the Namurian IVFs and the late-Quaternary examples employed for derivation of empirical relationships, the largest values of valley-fill thickness and width along the valley reach are recorded. For the Quaternary examples where the 3D geometry of the valley fills could be constrained closely (e.g., in high-resolution seismic data), these values are more likely to represent true, rather than apparent measurements (see details in Wang et al., 2019).

Statistical analyses

Statistical analyses have been performed in SPSS Statistics 25 and Minitab 18. The regression analysis and computation of the prediction of drainage areas have been performed in SPSS Statistics 25. Statistical analyses have also been carried out to investigate relationships between continuous variables. Pearson or Spearman correlation coefficients (R and r hereafter) are utilized to quantify linear and monotonic relationships, respectively, between pairs of continuous variables. Their statistical significance is expressed by P-values (P hereafter). P-values are compared with significance levels (α hereafter) that equal 0.05 or 0.1. Further explanation of statistical methods can be found in Davis (2002) and James et al. (2013).

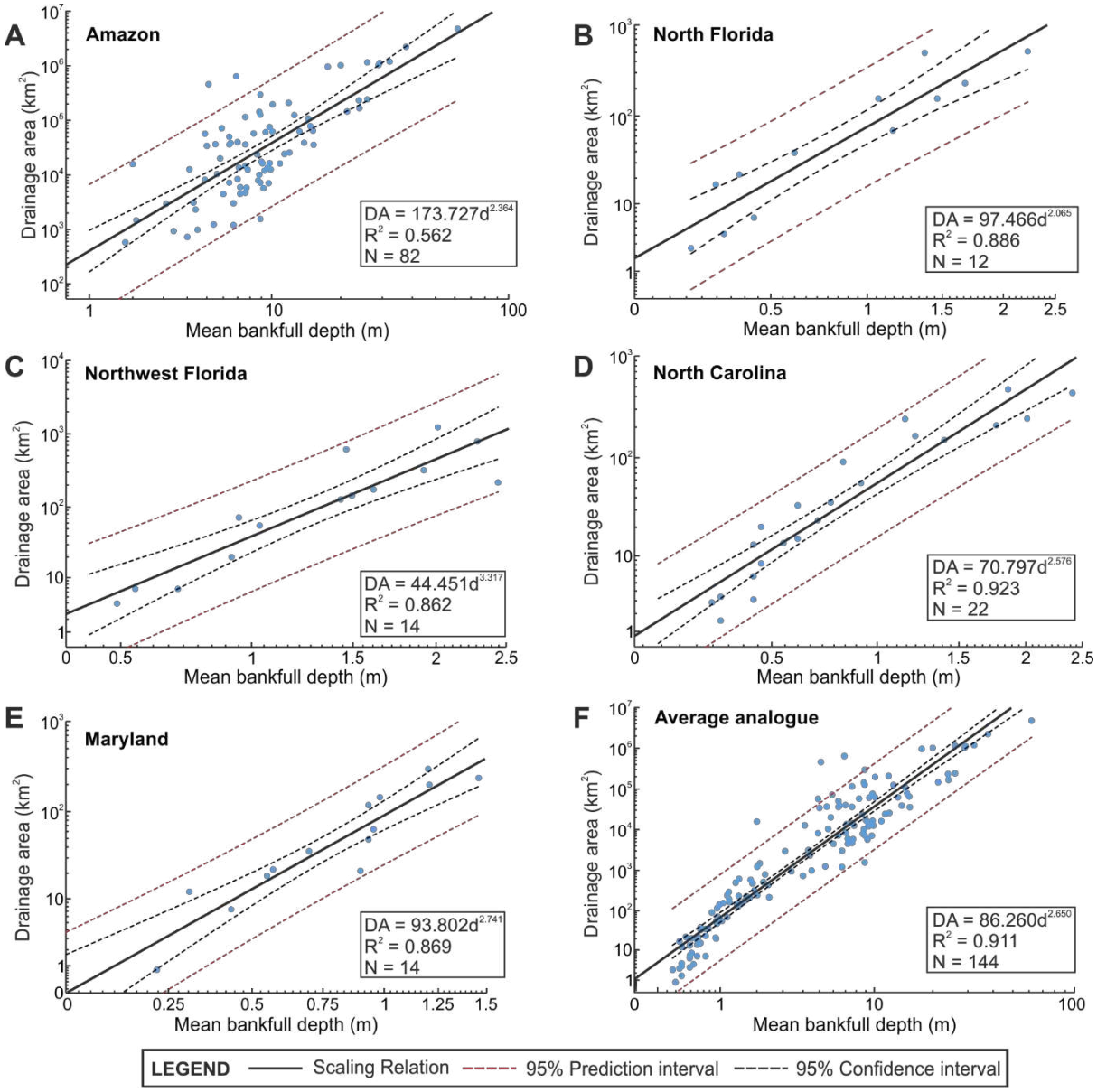

Fig. 3. Cross-plots of drainage area *versus* mean bankfull depth for selected modern analogues: Amazon basin(A), north Florida (B), northwest Florida (C), North Carolina (D), Maryland (E), and the cumulative dataset from all these modern analogues (F). Data in (B-E) are available in Davidson and North (2009). Original data taken from Beighley and Gummadi (2011), Metcalf (2004), Metcalf and Shaneyfelt (2005), Sweet and Geratz (2003) and McCandless (2003). 'N' denotes the number of readings. The results of regression analysis between these two variables (power-law relationship and R^2) are reported in respective boxes.

RESULTS

Facies proportions in incised-valley fluvial deposits

Data on the proportions of facies types can provide information on the relative predominance of types of depositional and post-depositional processes and of possible formative bedforms, which themselves might relate to river-discharge characteristics and drainage-area size. Database outputs on facies proportions in fluvial deposits of each IVF are presented in **Fig. 5**. When distributions in facies proportions in fluvial deposits across all the studied IVFs are considered (**Fig. 6**), it is noted that planar cross-stratified sandstones (mean

proportion: avgP = 0.40) and trough cross-stratified sandstones (avgP = 0.19) are the most abundant types of facies.

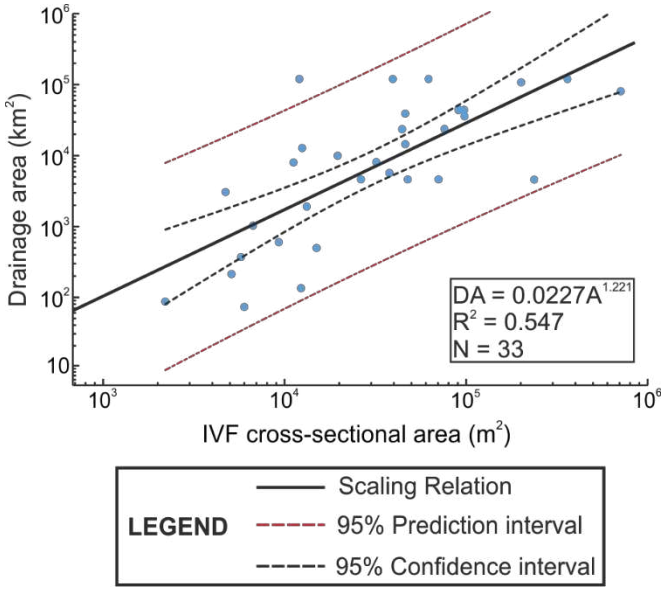

Fig. 4. Cross-plots of drainage area *versus* reconstructed IVF cross-sectional area for late-Quaternary incised-valley fills along passive continental margins. Data taken from Wang et al. (2019). 'N' denotes the number of readings. The results of regression analysis between these two variables (power-law relationship and R^2) are reported.

Distribution of cross-set thickness in incised-valley fluvial deposits

Figure 7 illustrates the distributions in the measured dune-scale cross-set thickness, from planar and trough cross-stratified sandstones or conglomerates in fluvial deposits of the studied IVFs. The results indicate that, for the studied IVFs, the mean values of the measured thickness of dune-scale cross-sets range from 0.32 ± 0.07 m (Aqueduct Grit IVF in North Wales; abbreviated as AGN hereafter; **Table 1**) to 1.94 ± 0.52 m (Lower Trent Sandstone IVF in the southern North Sea; LTSS). The coefficients of variation of cross-set thickness in the fluvial deposits of the studied IVFs are calculated and illustrated in **Fig. 8**. The results indicate that all the estimated values of CV (d_{st}) for the studied IVFs are lower than 0.88. Only two IVFs (Chatsworth Grit, East Midlands Shelf; Midgley Grit, Pennine Basin) are reported to have CV (d_{st}) within the range of 0.58 to 1.18 (0.61 and 0.78, respectively), and therefore to yield cross-set thickness statistics suitable for derivation of mean formative-dune height (Bridge and Tye, 2000). Values of CV (d_{st}) for all the other IVFs are below 0.58 (**Fig. 8**). This means that the values of CV (d_{st}) of cross-set thickness for most IVFs studied in this work do not meet the premise on which the empirical equation for flow-depth estimation of Leclair and Bridge (2001) (CV (d_{st}) = 0.88 ± 0.3, Fig. 8) is said to be applicable. Notwithstanding, this empirical equation has been tentatively applied in this work to all the studied IVFs (cf. Buller et al., 2018). This was done in absence of a more valid alternative, since estimation of flow depth based on story-thickness analysis is not practicable for the fluvial deposits of most of the studied examples, which are commonly characterized by amalgamated multistorey architectures and thus limited preservation of the full profile of barform or channel-fill elements. Estimations of drainage-basin areas based on depth estimations derived from measured cross-set thickness have been complemented with independent estimations based on IVF dimensions.

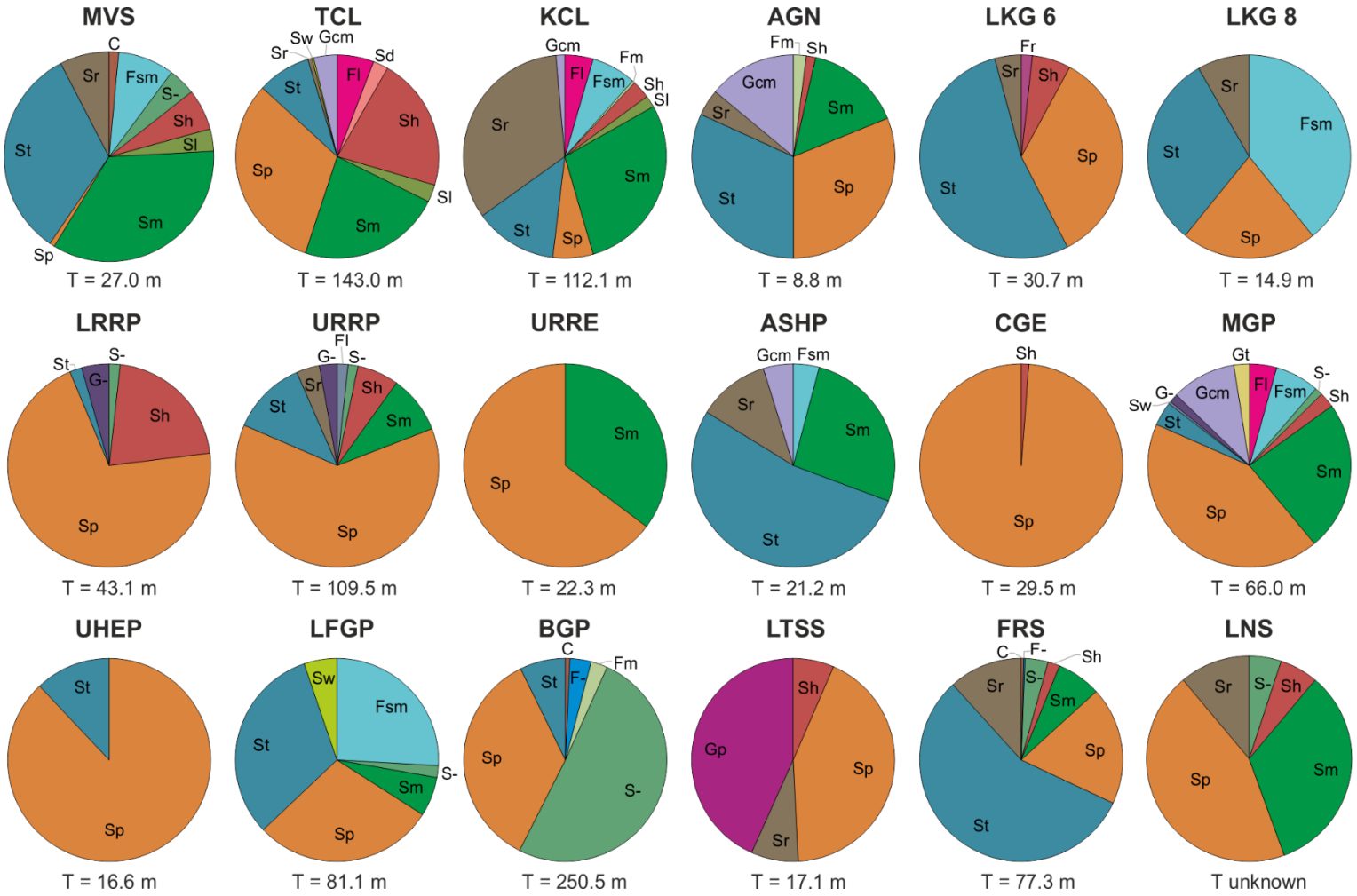

Fig. 5. Proportions of facies types in fluvial deposits of the studied IVFs. T denotes the sum of the thickness of all measured facies units for each incised-valley fill. See Table 2 for facies codes.

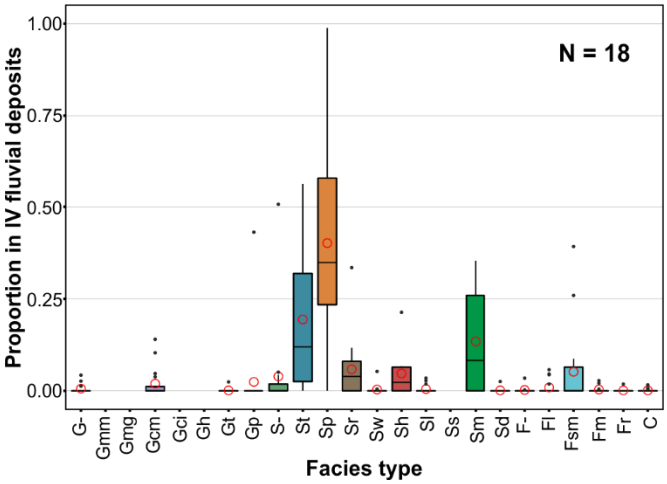

Fig. 6. Box plots that present distributions in facies proportions in fluvial deposits across the studied incised-valley (IV) fills. For each box plot, boxes represent interquartile ranges, red open circles represent mean values, horizontal bars within the boxes represent median values and black dots represent outliers (values that are more than 1.5 times the interquartile range). 'N' denotes the number of studied incised-valley fills. See Table 2 for facies codes.

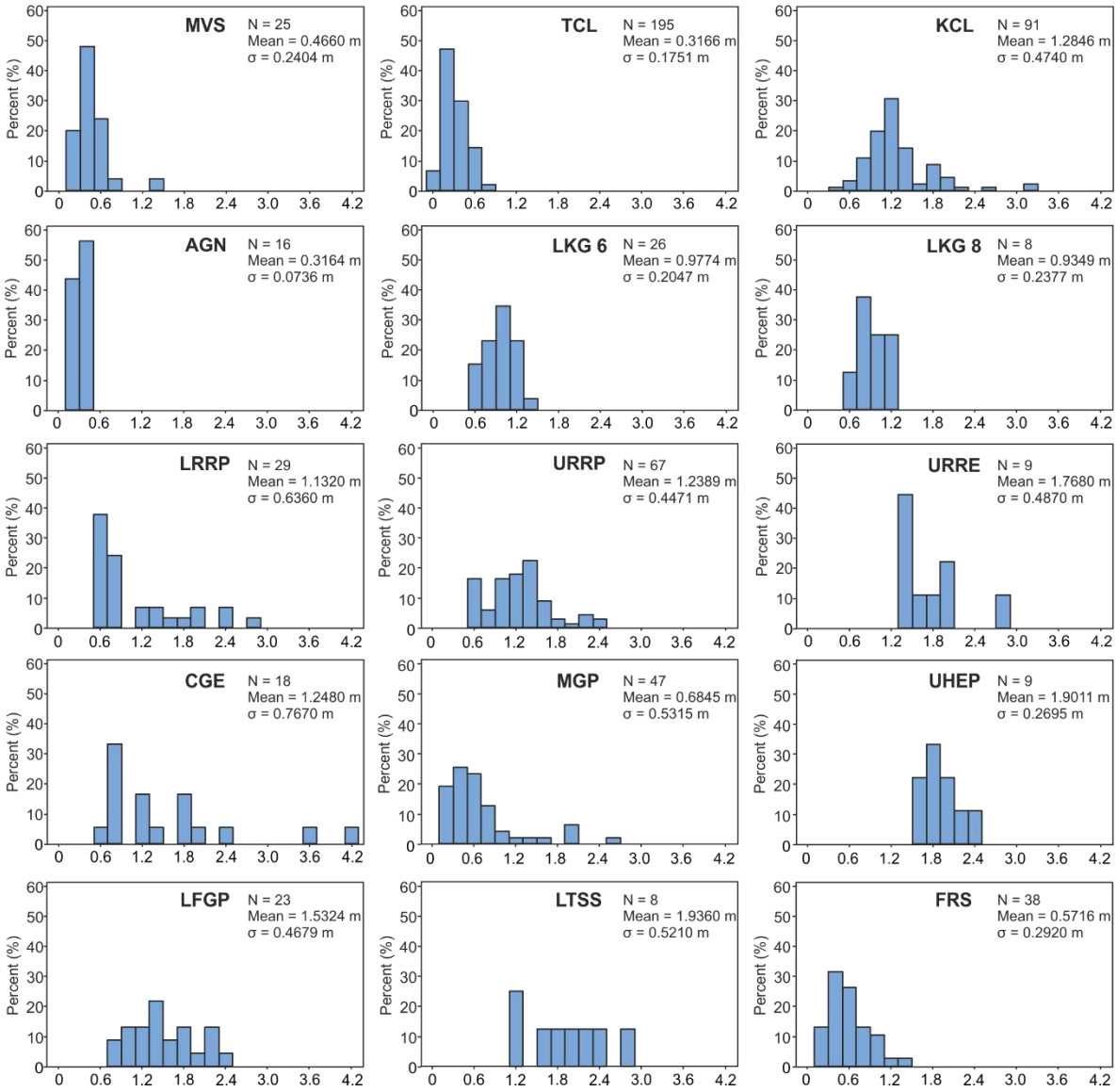

Fig. 7. Histograms that present distributions in the measured thickness of dune-scale cross-sets, from planar and trough cross-stratified sandstones and conglomerates in fluvial deposits of each IVF. 'N' denotes the number of readings and 'σ' denotes the standard deviation.

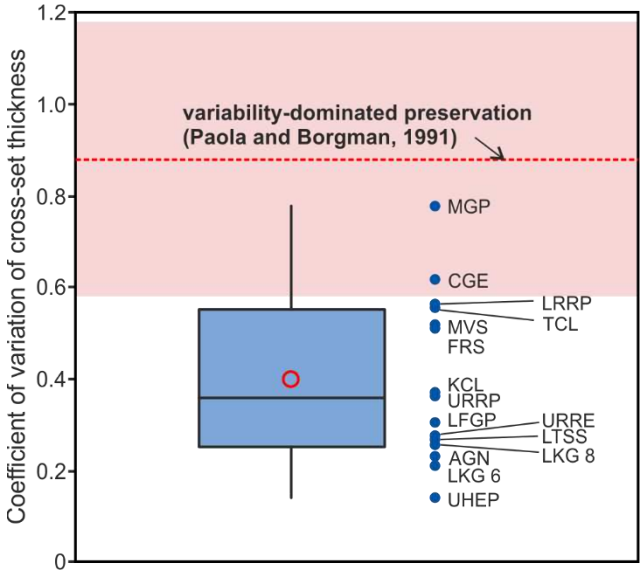

Fig. 8. Box plot of the distribution in the coefficient of variation of measured cross-set thickness for 15 IVFs. Individual values are also shown next to the boxplot for each IVF. For the boxplot, boxes represent interquartile ranges, red open circles represent mean values, horizontal bars within the boxes represent median values, and black dots represent outliers (values that are more than 1.5 times the interquartile range). The pink band indicates the 0.58-1.18 range, wherein data are considered suitable for calculating mean dune height, according to the method of Bridge and Tye (2000). The red dashed line denotes the value indicated by the variability-dominated preservation model of Paola and Borgman (1991).

Estimation of formative flow depth

Estimation of mean bankfull depth for the formative rivers of the studied IVFs from measured cross-set thickness is represented in **Fig. 9**. The results indicate that the estimated mean bankfull depth of these rivers ranges from 6 to 38 m, with an average value of 21 m. The estimated mean bankfull depth for the formative rivers of the Farewell Rock (FRS), Spireslack Sandstone (MVS), Tullig Sandstone (TCL) and Aqueduct Grit (AGN) IVFs is smaller than or equal to 10 m. The estimated mean bankfull depth for IVFs of the Upper Rough Rock of the East Midlands Shelf (URRE), Upper Howgate Edge Grit (UHEP) and Lower Trent Sandstone (LTSS) is larger than 30 m. The mean bankfull depths estimated for rivers draining into the Pennine valleys range from 13 m to 38 m.

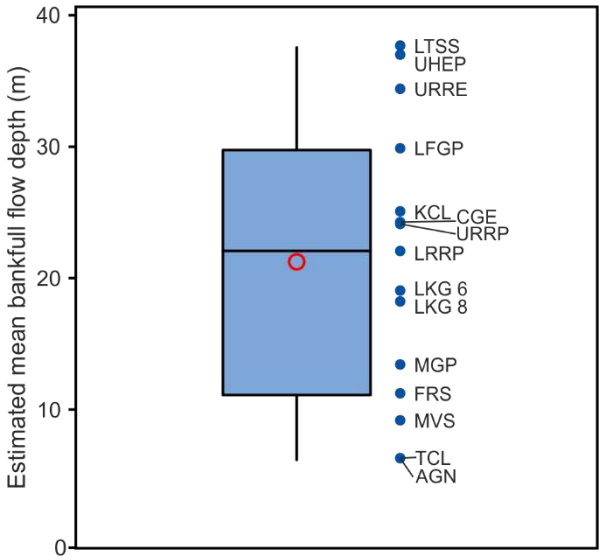

Fig. 9. Box plot of the distribution in the estimated mean bankfull depth for 15 incised-valley fills considered in this work. Individual values are also shown next to the boxplot for each incised-valley fill. For the boxplot, boxes represent interquartile ranges, red open circles represent mean values, horizontal bars within the boxes represent median values, and black dots represent outliers (values that are more than 1.5 times the interquartile range).

In the fluvial deposits of the studied IVFs, recognition of bar and channel-fill elements whose vertical profile is completely preserved is limited, since these units are commonly amalgamated laterally and vertically to form multistorey architectures. For the

very few cases where complete bar and channel-fill elements are recognized, estimates of maximum bankfull depth can be attempted by assuming a compaction factor of 10% (after Ethridge and Schumm, 1978), which yield values of 6.1 m, 4.0 m, 8.6 m and 6.2 m for the Spireslack Sandstone (MVS), the Tullig Sandstone (TCL), the Midgley Grit (MGP) and the Chatsworth Grit (CGE) respectively. It is significant that the projected values of mean bankfull depths based on these maximum bankfull depths (obtained assuming the channel cross-sectional area approximated by a half-elliptical shape, and hence the mean bankfull depth as being equal to $\pi/4$ times the maximum bankfull depth) are consistently smaller than the mean bankfull depths estimated from measured cross-set thickness.

Estimation of drainage area

Two independent approaches are employed to estimate the drainage areas for the studied IVFs. The first method is based on the empirical equations that use measured mean cross-set thickness (S_m) to estimate mean dune height (h_m), itself used to derive values of mean bankfull depth (d_m) that can be applied to regional curves to predict catchment size. The second method employs scaling relationships between IVF dimension and drainage area (**Fig. 4**), based on a compilation of data from late-Quaternary examples (Wang et al., 2019).

As the original published datasets vary significantly with respect to the availability of data on cross-set thickness and IVF dimension, both methods for the estimation of drainage areas can only be applied simultaneously to eight IVFs. The method based on the measured dune-scale cross-set thickness is applied to fifteen IVFs, whereas the method based on IVF dimension is applied to ten IVFs (**Fig. 10**).

The results of estimated drainage areas for the studied IVFs are represented in **Fig. 10.** Estimations of drainage area based on the northwest Florida and Maryland coastal-plain analogues are larger than the value obtained using the Amazon basin as analogue, whereas predicted values of drainage area based on the North Carolina and north Florida coastal-plain analogues are smaller than that based on the Amazon regional curve (**Fig. 10A**). The orders of magnitude of drainage-area size for the studied IVFs range from 10^3 km^2 to 10^6 km^2, but prediction intervals cover a wider range, from 10^3 km^2 to the order of 10^7 km^2. Estimations of the size of drainage areas based on the average modern analogue range in order of magnitude from 10^4 km^2 to 10^6 km^2 (**Fig. 10B**). The estimated drainage areas for the Farewell Rock (FRS), Spireslack Sandstone (MVS), Tullig Sandstone (TCL) and Aqueduct Grit (AGN) IVFs are in the order of 10^4 km^2; only three IVFs (URRE, UHEP, LTSS) have estimated drainage areas in the order of 10^6 km^2. For all eight IVFs with available data on both dune-scale cross-set thickness and IVF dimension, the 95% prediction intervals of the two approaches to catchment size estimation overlap significantly (**Fig. 10B**); the predictions of each of these two methods fall within the prediction interval of the other method, except for one case (MGP). For the Farewell Rock (FRS) and Chatsworth Grit (CGE) IVFs, the two alternative approaches return broadly similar values (50,887 km^2 *versus* 47,547 km^2 for FRS; 402,564 km^2 *versus* 525,819 km^2 for CGE). Estimations of drainage-basin area obtained with the two approaches do not vary in a systematic way: values derived from one approach are not systematically larger or smaller than those obtained with the other method (**Fig. 10**). Base-case predictions of drainage areas based on these two methods are not correlated ($R = -0.163$, $p = 0.700$).

Facies architecture in incised-valley fluvial deposits and drainage-basin size

Considering that the manner in which river systems are expected to respond to flood waves and undergo modulation of water discharge depends in part on the size of their drainage areas (Syvitski et al., 2003; Sømme et al., 2009; Hansford et al., 2020), relationships

are investigated between the size of the drainage-basin areas of each IVF, as estimated from data on dune-scale cross-set thickness, and both the proportion of selected facies types in incised-valley fluvial deposits (**Fig. 11**) and cross-set thickness variability (**Fig. 12**). For scopes of analysis, certain facies types are grouped together according to the possible flow regime of their formative bedforms (lower *versus* upper-flow regime, and possible transition between them).

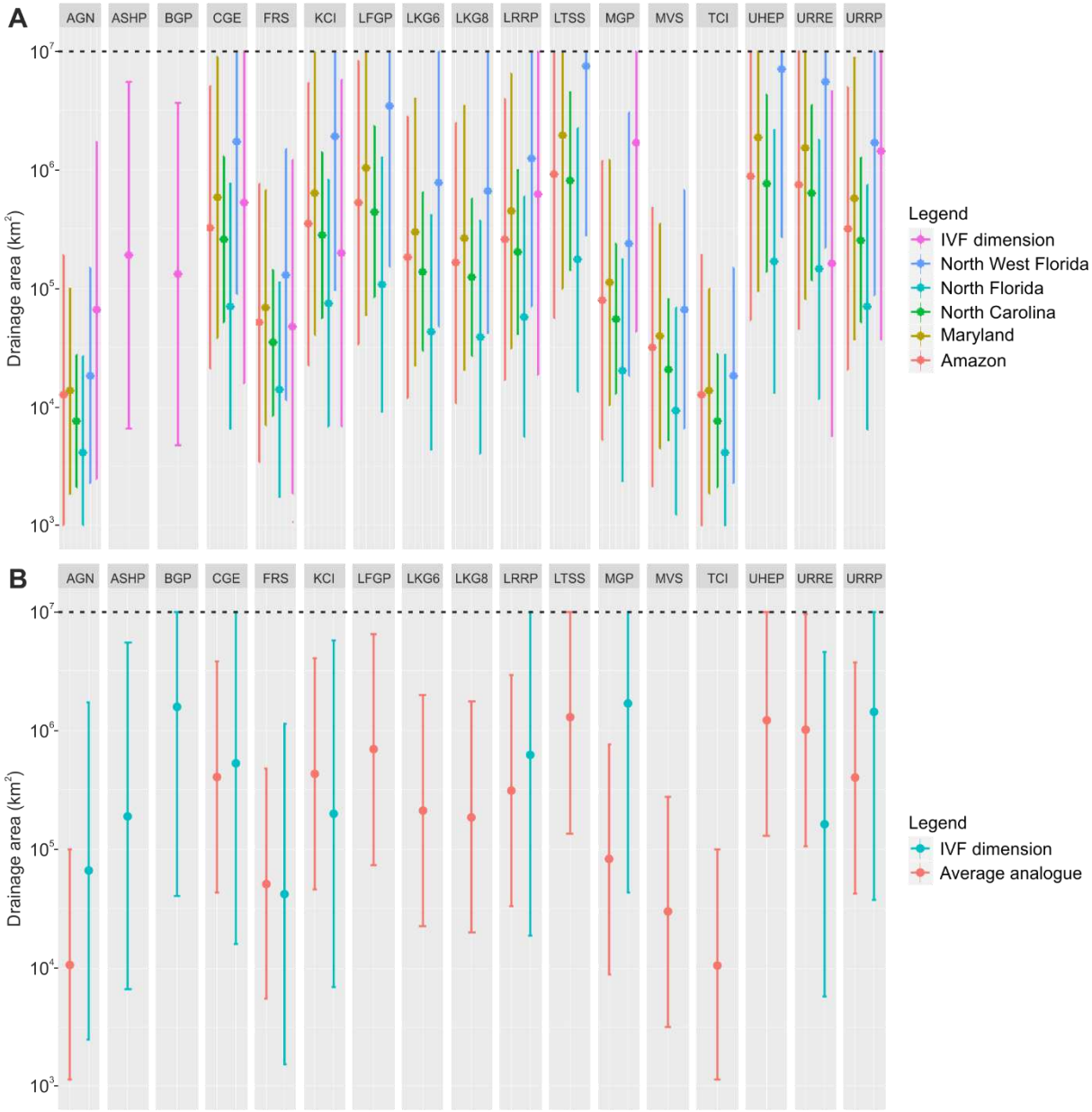

Fig. 10. Range plots of estimated drainage area from measured cross-set thickness and IVF dimension. Solid dots represent the predicted values; vertical bars represent 95% prediction intervals. Note that prediction intervals are truncated at 10^7 km^2, since it is deemed unrealistic that the studied Namurian IVFs could be fed by drainage areas larger than this value, based on palaeogeographic considerations.

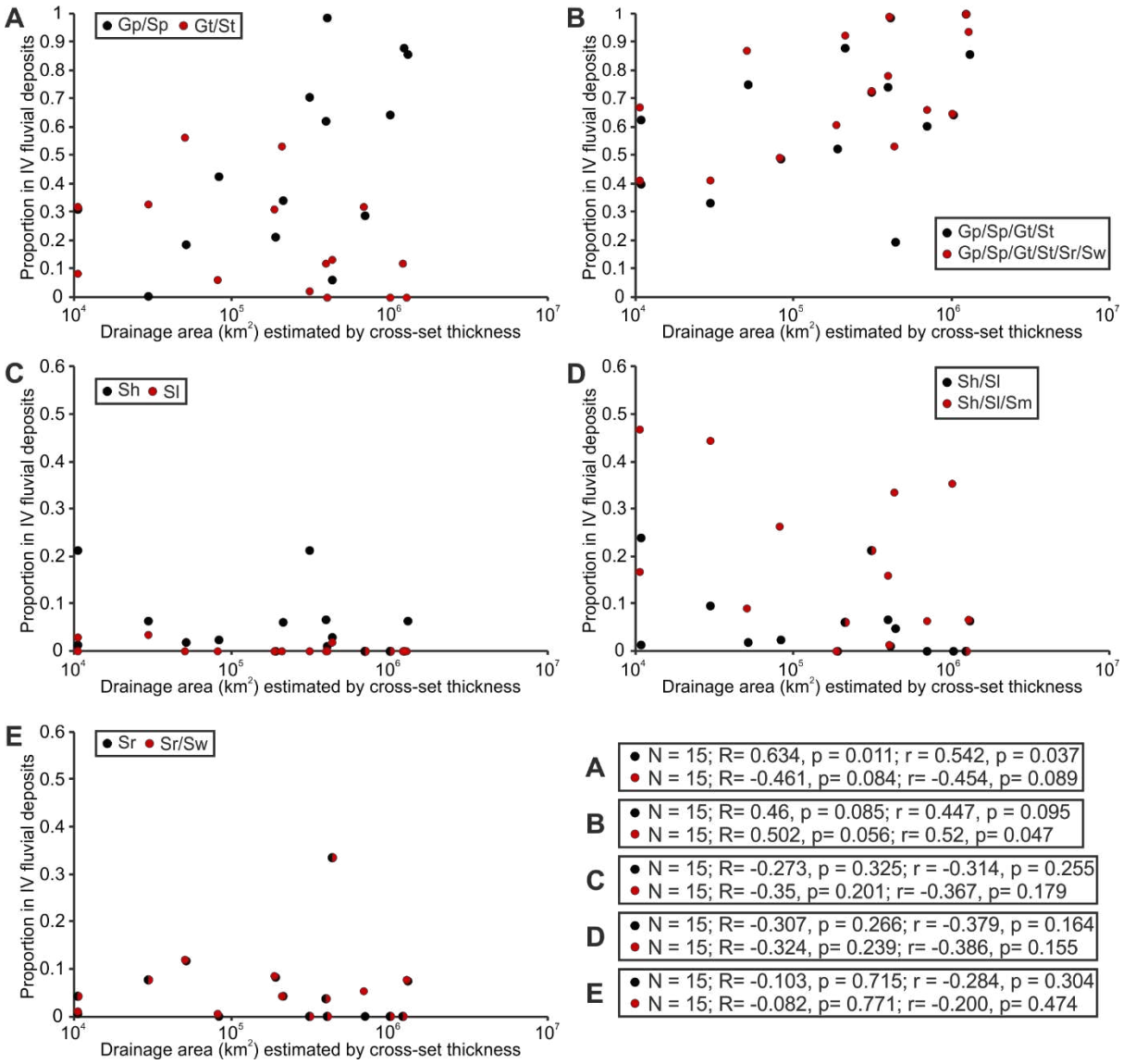

Fig. 11. Cross-plots of proportions of facies types within fluvial deposits of the studied incised-valley fills *versus* drainage areas estimated from mean cross-set thickness of each. (A) Cumulative proportions of facies Gp and Sp, and of facies Gt and St *versus* drainage area. (B) Cumulative proportions of facies Gp, Sp, Gt and St and of facies Gp, Sp, Gt, St, Sr and Sw *versus* drainage area. (C) Proportions of facies Sh and Sl *versus* drainage area. (D) Cumulative proportions of facies Sh and Sl and of facies Sh, Sl and Sm *versus* drainage area. (E) Proportion of facies Sr and cumulative proportions of Sr and Sw *versus* drainage area. Half-and-half dots represent IVFs for which the two proportions are the same. For each pair of variables, the correlation coefficients and p-values are reported in respective boxes on the bottom right. 'N' denotes the number of readings, 'R' denotes Pearson's R, and 'r' denotes Spearman's rho.

A positive correlation is noted between the cumulative proportion of planar cross-stratified sandstones and conglomerates (Gp/Sp) in incised-valley fluvial deposits and the estimated drainage area (**Fig. 11A**). A moderate negative correlation is noted between the cumulative proportion of trough cross-stratified sandstones and conglomerates (Gt/St) and the estimated drainage area, but this is not statistically significant (**Fig. 11A**).

When Gp, Sp, Gt and St facies are considered jointly, a moderate positive relationship is seen between the cumulative proportion of these facies and the estimated drainage area, but

this is not statistically significant (**Fig. 11B**); when Gp, Sp, Gt, St, Sr (current ripple-laminated sandstones) and Sw (wave ripple-laminated sandstones) facies are considered together, a moderate positive correlation is seen between the cumulative proportion of these facies and the estimated drainage area (**Fig. 11B**).

A weak and not statistically significant negative correlation is noted between the proportion of planar laminated sandstones (Sh) or of low-angle cross-stratified sandstones (Sl) and the estimated drainage area (**Fig. 11C**). No apparent correlation is noted between the proportion of low-angle cross-stratified sandstones (Sl) and the estimated drainage area (**Fig. 11C**).

When Sh and Sl facies are considered jointly, a weak and not statistically significant negative relationship is seen between the cumulative proportion of these facies and the estimated drainage area (**Fig. 11D**); when Sh, Sl and Sm (massive sandstones) facies are considered together, a weak and not statistically significant negative correlation is noted between the cumulative proportion of these facies and the estimated drainage area (**Fig. 11D**).

No correlation or a very weak correlation is identified between the proportion of current ripple-laminated sandstones (Sr) and the estimated drainage area (**Fig. 11E**); when Sr and Sw are considered jointly, no correlation or a very weak correlation is noted between their cumulative proportion and the estimated drainage area (**Fig. 11E**).

A moderate negative relationship is noted between the coefficient of variation of dune-scale cross-set thickness and the size of drainage areas estimated from cross-set thickness (**Fig. 12A**), whereas a moderate positive relationship is noted between the coefficient of variation of cross-set thickness and the size of drainage areas estimated from IVF dimension, albeit not statistically significant at the level of 0.1 (**Fig. 12B**).

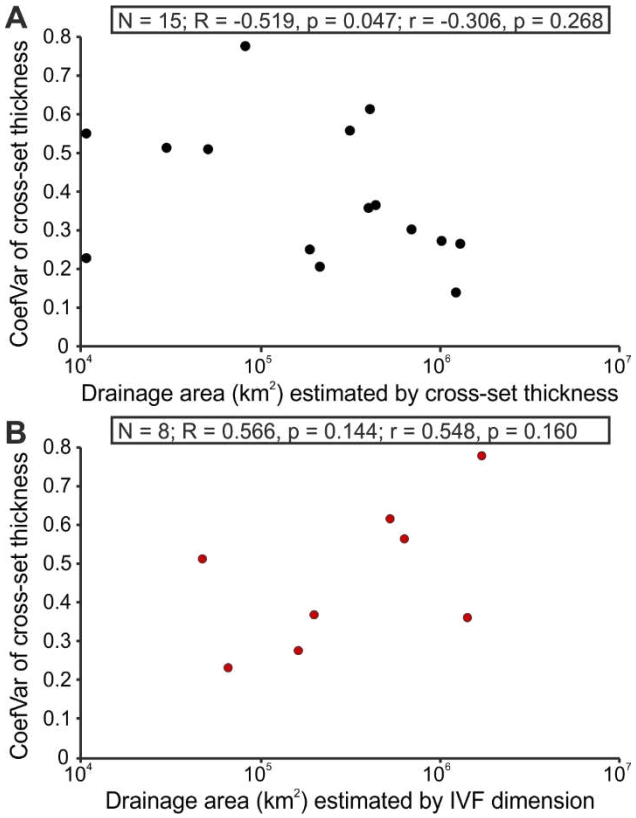

Fig. 12. Cross-plots of the coefficient of variation of cross-set thickness *versus* (A) drainage area estimated by cross-set thickness and (B) drainage area estimated by IVF dimension. For each pair of variables, the correlation coefficients and p-values are reported in respective boxes. 'N' denotes the number of readings, 'R' denotes Pearson's R, and 'r' denotes Spearman's rho.

DISCUSSION

Palaeohydrological characteristics

Discharge variability can exert a primary control on alluvial stratigraphy, from bedform to basin scales (Fielding et al., 2009 and 2018; Plink-Björklund, 2015; Nicholas et al., 2016; Trower et al., 2018; Colombera and Mountney, 2019; Ganti et al., 2019b; Leary and Ganti, 2020). Perennial rivers with low discharge variability are typically characterized by the predominance of Froude subcritical bedforms (preserved as cross-stratification and ripple cross-lamination) and subordinance of Froude supercritical and transcritical bedforms (preserved as planar lamination and low-angle cross-stratification; cf. Fielding et al., 2009, 2018; Plink-Björklund, 2015; Colombera and Mountney, 2019). In the fluvial deposits of the studied IVFs, the predominance of sandstones with planar and tabular cross stratification and ripple cross lamination (**Fig. 5** and **Fig. 6**), consistent with what is generally represented in classical facies models for sandy river channel deposits (e.g., Walker, 1976; Collinson, 1996; Miall, 1996; Bridge, 2006), supports the notion that the palaeoriver-systems feeding the Namurian IVFs of the UK and Ireland were perennial and characterized by relatively low discharge variability (i.e., they lacked the flow variability typical of some subtropical rivers that are more prone to experience conditions of upper flow regime; cf. Fielding et al., 2009, 2018; Plink-Björklund, 2015). This interpretation is reconciled with the inference of a predominantly equatorial humid tropical climate prevailing in the study areas during the Namurian (Davies, 2008; Davies et al., 2012; Boucot et al., 2013; Blakey, 2016). Based on global quantitative analyses of modern river discharge variability and hydrograph shape with respect to climate types, Hansford et al. (2000) indicated that due to intense perennial precipitation, rivers in tropical rainforest climate are typically characterized by large discharge, low discharge variability and broad flood hydrographs, whereby the flood discharge tends to build slowly and decline gradually over the course of several months.

If the studied Namurian palaeorivers were indeed hydrologically similar to these modern tropical rivers, it could be hypothesized that a signature of their hydrology might be preserved in their dune-scale cross-stratification. Values of the coefficient of variation of measured cross-set thickness for the studied Namurian incised-valley fluvial deposits are consistently lower than what is expected for steady flow state, based on theoretical, experimental and numerical studies (e.g. Paola and Borgman, 1991; Bridge and Tye, 2000; Leclair and Bridge, 2001; Leclair, 2002; Jerolmack and Mohrig, 2005; Ganti et al., 2013) (**Fig. 8**). Given the reconstructed scale and hydrodynamics of the studied river systems, low inter-annual discharge variability is expected for these rivers, raising the question as to whether this may be responsible for the observed low values of CV (d_{st}). One possible explanation might be that, for the studied palaeorivers, cross-set-forming dunes tended to accumulate their deposits under limited disequilibrium, and in a way whereby the low variability in cross-set thickness would merely reflect the limited variability in magnitude across different flood events. However, conditions of bedform equilibrium and low discharge variability may not best explain these observations. Theoretical analyses and flume experiments under steady and unsteady flows by Leary and Ganti (2020) indicate that preserved fluvial cross strata tend to record bedform evolution during flood recession. Given a characteristic bedform disequilibrium timescale $T^* = Tf / Tt$, where Tf is the duration of the prevailing flow and Tt is the bedform adjustment timescale (Myrow et al., 2018), broad flood hydrographs, having a gradual decline in discharge and $T^* \geq 1$, tend to result in values of CV (d_{st}) ≈ 0.88, whereas flashier flood hydrographs, with rapid decreases in flood discharge and $T^* \ll 1$, tend to result in CV (d_{st}) values markedly lower than 0.88 (Leary and Ganti, 2020).

The cross-set thickness variability can therefore act as an indicator of disequilibrium in the sedimentary record and yield information on the relative timescales of formative flood variability and bedform adjustment (Leary and Ganti, 2020). In this perspective, the low variability (coefficients of variation) of cross-set thickness for the studied Namurian incised-valley fluvial deposits could be attributed to bedform disequilibrium relative to formative flows. Large, low-gradient perennial rivers draining tropical regions exist that experience phases of flood recession that are sufficiently rapid relative to their timescale of bedform turnover, which tend to cause bedform disequilibrium and high bedform preservation. This is observed in the Amazon, the Congo, and the Paraná, for example (Leary and Ganti, 2020), i.e., in rivers whose hydrology is affected to some extent by seasonal and interannual variations in rainfall, partly due to monsoonal circulation in sectors of their catchments (Liebmann and Mechoso, 2011; Materia et al., 2012; Syvitski et al., 2014). The Namurian palaeorivers investigated in this study may have had a similar behaviour, possibly in relation to the role of monsoons in shaping flood hydrographs modulated by water discharge from rainforests. For rivers receiving a mixed water supply from tropical rainforest and monsoon zones, the shape of flood hydrographs tend to be similar to the patterns characterized in monsoonal rivers, i.e., rapid rise and rapid fall of flood stage, whereas the discharge variability may remain low as the perennial precipitation can moderate the floods in amplitude (cf. Plink-Björklund, 2015; Hansford et al., 2020). Although palaeofloral observations indicate a generally equitable climate for low-latitude regions during the Carboniferous, and particularly in Namurian times (Chaloner and Creber, 1990; Falcon-Lang and Scott 2000; and references therein), geological evidence and palaeogeographic considerations suggest that some seasonality and conditions conducive to monsoonal circulation might have occurred in parts of the drainage areas of the studied palaeorivers (Broadhurst et al., 1980; Rowley et al., 1985; Parrish, 1993; Falcon-Lang, 2000; Bijkerk, 2014). Whether monsoon-driven seasonal flood regimes might partly explain aspects of the facies architecture of these Namurian valley fills is a topic that warrants further investigation (cf. Ventra et al., 2015a, 2015b; Kane and Hodgson, 2015).

The values of mean bankfull depth for the formative rivers of the studied IVFs estimated from mean values of measured dune-scale cross-set thickness ranges from 6 m to 38 m, with an average of 21 m (**Fig. 9**). However, for few examples (MVS, TCL, MGP, CGE) studied in this work, where complete bar and channel-fill elements in incised-valley fluvial deposits can be recognized, the values of mean bankfull depths estimated from measured cross-set thickness are consistently larger than the values derived from complete bar and channel-fill elements. Furthermore, in some cases (LRRP, URRE, UHEP, LTSS) values of maximum bankfull depths projected from the mean bankfull depths (themselves estimated from mean cross-set thicknesses) are even larger than the restored thickness of the IVFs themselves, even assuming a compaction factor of 10%. In addition, the fluvial deposits of the studied IVFs are commonly characterized by multistorey architectures (Hampson et al., 1997; Hampson et al., 1999; Davies et al., 1999), and this should support the idea that the fluvial fill of each of these valleys should be significantly thicker than the palaeodepth of the river that formed it. These inconsistencies might arise in part because flow depth estimated from mean cross-set thickness tends to yield an overestimation of the mean bankfull depth, due to preferential preservation of thicker dune-scale cross-sets in portions of channel deposits that represent deeper channel areas (Holbrook and Wanas, 2014), and perhaps because estimation of dune height from cross-set thickness has been attempted in this work despite the fact that the values of CV (d_{st}) of most IVFs studied in this work do not meet the premise on which the empirical equation of Leclair and Bridge (2001) is said to be applicable

(i.e., CV (d_{st}) = 0.88 ± 0.3, **Fig. 8**). Misidentification of cross-sets that represent the preserved product of unit bars (Reesink, 2019) or of bedforms that developed under conditions of upper flow-regime or at the transition to the upper flow-regime, as dunes, is another possible explanation. Furthermore, the scaling between dune height and flow depth is influenced by flow regime, controlling where dunes sit on the bedform stability field, and determining an increase in height from the transition from ripple or lower-stage plane beds to a maximum in the middle of the dune field, followed by a decrease to near zero at the transition to the upper-stage plane beds (Bridge and Tye, 2000). Estimations of flow depth larger than the restored thickness of IVFs might also be attributed in part to the fact that IVF fluvial strata are prone to be truncated at the top by wave or tidal ravinement (e.g., O'Mara et al., 1999; Wignall and Best, 2000; George, 2001; Brettle et al., 2002; cf. Wellner and Bartek, 2003; Wang et al., 2020). Finally, high bedform preservation related to rapid falling stages of formative floods could be an alternative explanation (Leary and Ganti, 2020), and this would be consistent with the observations presented above relating to the coefficients of variation of cross-set thickness.

Upstream controls on the facies architecture of incised-valley fluvial deposits

Considering similar prevailing humid tropical climate conditions for the studied IVFs, negative relationships between estimated drainage area and the proportions of facies that were possibly deposited under upper-flow-regime or transitional to upper-flow-regime conditions (planar laminated, low-angle cross-stratified and massive sandstones), as well as positive relationships between drainage area and proportions of facies that were likely deposited under lower-flow-regime conditions (planar cross-stratified, trough cross-stratified and ripple-laminated sandstones or conglomerates) (**Fig. 11**), might reflect the fact that the size of drainage-basin areas could leave a distinguishable record in the facies architecture of fluvial deposits within incised valleys through its control on variability in water discharge (cf. Colombera and Mountney, 2019). Based on global quantitative analyses of modern rivers, Hansford et al. (2020) indicated that water discharge variability associated with the occurrence of extreme meteorological events, quantified by DVI_y and $Q_{99.863}/Q_{50}$, tends to decrease with increasing drainage areas. This is attributed to the fact that smaller and steeper drainage basins are more prone to larger differences between flood and base-flow discharge (Smith, 1992; Robinson and Sivapalan, 1997; Sømme et al., 2009) as external flood drivers (e.g., storms) are more likely to affect the entire drainage basin. However, correlations between estimated drainage area and the proportions of facies that were possibly deposited under transitional to upper-flow-regime conditions (planar laminated, low-angle cross-stratified and massive sandstones) are commonly weak or non-existent (Fig. 11C and D). This is contrary to what may be typically expected, but consistent with recent quantifications highlighting a limited effect of drainage-basin size on discharge variability (Hansford et al., 2020). In part, this discrepancy might also arise because of variability in the origin of these facies types and of the associated uncertainty in interpretations. Planar laminated and low-angle cross-stratified sandstones could possibly have been deposited as lower-flow-regime plane beds as well as through migration of bedforms in the upper flow-regime or at the transition to the upper flow-regime (parallel laminations and convex-up low-relief bedforms). Massive sandstones can also be post-depositional in origin (Colombera and Mountney, 2019) and can contain faint or non-visible laminations (cf. Hamblin, 1965).

The negative correlation between the coefficient of variation of cross-set thickness *versus* the size of drainage areas estimated from mean values of cross-set thickness (**Fig. 12A**) might reflect how river systems with drainage areas of different sizes respond to flood

and modulate water discharge (e.g., in terms of inter-annual discharge variability), since these factors potentially control the preservation of cross strata. In consideration of the potential control of river discharge variability on resulting alluvial stratigraphy (Fielding et al., 2018), the relationship between metrics of discharge variability and the size of drainage areas is examined for modern rivers (**Fig. 13**), in order to derive insight that could be applied to IVFs in the rock record. To characterize inter-annual discharge variability, Fielding et al. (2018) proposed to use the coefficient of variation of annual peak flood discharge CVQp. To characterize discharge variability from the annual to inter-annual scale, Hansford et al. (2020) proposed instead the use of an index of yearly discharge variability (DVI_y), equal to the average of the difference between the highest and the lowest daily discharge in the same year divided by the average discharge across many years. Based on daily discharge data reported in Fielding et al. (2018), a moderate negative relationship is seen between CVQp and drainage area for 26 modern rivers distributed across different climatic zones (**Fig. 13**). Similarly, based on discharge data from Hansford et al. (2020), relating to 575 gauging stations from 490 rivers located in any climates, a weak negative relationship is observed between DVI_y and drainage area (regression with $R^2 = 0.22$). However, when the same analyses are restricted to rivers from rainforest climatic zones, based on daily discharge data by Hansford et al. (2020), no correlation is noted between the coefficient of variation of peak discharge (CVQp) and catchment size (**Fig. 13**), but stronger negative correlation is seen between DVI_y and catchment size ($R^2 = 0.39$; negative correlation of the same strength is also seen for these two variables when considered for the data pool of persistent rivers: $R^2 = 0.39$). Overall, this indicates that (i) the degree of catchment integration acts as a control on inter-annual discharge variability, but its role may be relatively limited, and (ii) whether the effect of catchment size on discharge variability is more or less pronounced for rivers from tropical rainforest climates cannot be established clearly, and appears to depend on how discharge variability is quantified.

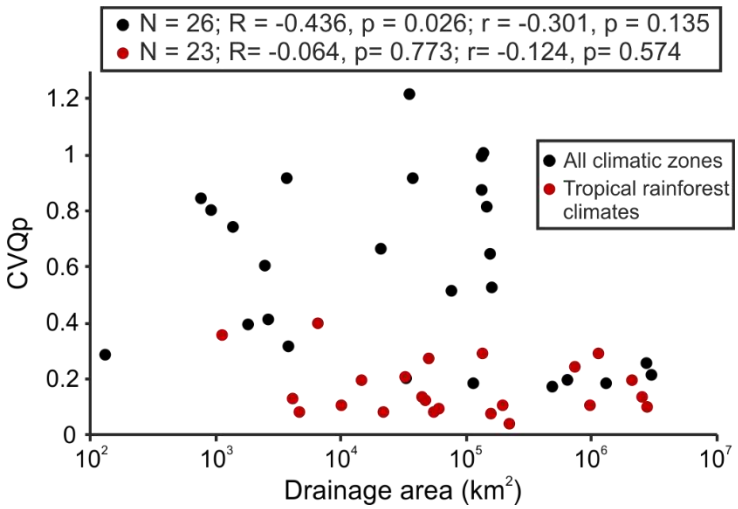

Fig. 13. Cross-plots of the coefficient of variation of annual peak discharge (CVQp) *versus* drainage area for modern rivers across all climate zones and in tropical rainforest climates, respectively. Black spots denote examples from all climatic zones with data taken from Fielding et al. (2018). Red spots denote examples in tropical rainforest climates with data taken from Hansford et al. (2020). For each pair of variables, the correlation coefficients and p-values are reported in respective boxes. 'N' denotes the number of readings, 'R' denotes Pearson's R, and 'r' denotes Spearman's rho.

Palaeogeographic reconstructions

Sedimentological data such as palaeocurrent vectors or palaeoslope indicators (e.g., interpreted movement directions of slumps, orientation of facies belts), provide information on directions of sediment transport, but tend to be affected by local topographic variations. Provenance studies based on detrital zircon age dating and heavy-mineral analyses can

provide key information on the source areas at a larger scale. The proposed estimations of the size of drainage areas form a dataset that can be used to integrate existing provenance and sedimentological data, to improve understanding of likely source areas, enable reconstruction of source-to-sink systems, and contribute to the refinement of regional palaeogeographic reconstructions for the Namurian (**Fig. 1** and **Fig. 14**). Implications of the results for selected basins (**Fig. 1**) are presented in the following section. The size of drainage areas for each IVF used for regional palaeogeographic reconstructions represents either (i) the average of the base-case predicted value estimated from the average modern analogue and that estimated from IVF dimension, or (ii) the value obtained with either of these two methods if data on cross-set thickness or IVF dimension are lacking.

Pennine Basin

The integration of heavy-mineral analysis and detrital-zircon dating for late Carboniferous sandstones of the Pennine Basin by Hallsworth et al. (2000) indicates that during the Namurian, the majority of sediment was derived from the north, with subordinate amounts of sediment supplied from the Wales-Brabant High, on the southern margin of the basin. The northern source areas lay within the part of Laurentia-Baltica affected by the Caledonian orogeny, which is considered to locate to the north of the present-day North Sea and has extended to present-day Greenland. Based on combined analyses of heavy minerals, garnet geochemistry and palaeocurrent directions of late Carboniferous (Yeadonian) fluvial sandstones in the Pennine Basin, Hallsworth and Chisholm (2008) proposed that the fluvial sandstones of the Rough Rock of the central Pennines were mainly supplied with sediment of northerly provenance. Additional local sediment sources can be inferred at the northern and southern basin margins and from an intrabasinal high, the Market Weighton High. The main north branch of the drainage system extended into the North Staffordshire area, whereas the south branch did not extend beyond the Widmerpool Gulf.

Estimations of drainage areas for the lower Rough Rock and Upper Rough Rock IVFs in the Pennine Basin (LRRP, URRP) and for the Upper Rough Rock IVF in the East Midlands Shelf (URRE) yield average predicted values of approximately 470,000 km^2, 910,000 km^2 and 590,000 km^2, respectively. Taking into account the studies on the provenance of the Rough Rock IVFs and the average value of base-case estimations of drainage areas based on the average modern analogue and IVF dimension, palaeogeographic maps that illustrate the possible Yeadonian drainage configurations have been proposed (**Fig. 14H and I**). The sum of the estimated drainage area for the URRP and URRE IVFs is used when reconstructing the palaeogeography. The estimated drainage areas are of a size that is compatible with the extent of the source terranes recorded by the detrital zircon age spectra and heavy-mineral analysis. The proposed reconstruction accommodates the hypothesis that the northern drainage system bifurcated into two branches because of the existence of a topographic high, the Market Weighton High (Hallsworth and Chisholm, 2008; Waters et al., 2009). The northern branch fed the Upper Rough Rock in northern England (URRP) and the Aqueduct Grit in North Wales (AGN); the southern branch diverted westwards due to the existence of the Wales-Brabant High on the south margin of the basin, as recorded in palaeocurrent data (Bristow, 1988; Hallsworth and Chisholm, 2008), and alimented the Upper Rough Rock in the Widmerpool Gulf (URRE).

Clare Basin

The provenance of Namurian sedimentary strata of the Clare basin remains highly contentious despite decades of research. Contrasting interpretations are derived on the basis

of sedimentological data, i.e., palaeocurrent indicators and interpreted movement directions of slumps: Collinson et al. (1991) envisaged a source from the west or northwest, whereas Wignall and Best (2000) suggested sediment influx from a southerly provenance. Based on detrital-zircon age data from three Namurian sandstone units (Ross Formation, Tullig Sandstone, Doonlicky Sandstone), Pointon et al. (2012) suggested that from the time of deposition of the uppermost Ross Formation (early Kinderscoutian) until the deposition of the Doonlicky Sandstone (late Kinderscoutian to early Marsdenian), a major sediment source (over 35%-40%) for the Clare basin was represented by a number of small terranes of Gondwanan affinity (Avalonia/Ganderia, Armorica and Iberia) located to the south; yet, it is recognized that the possibility of a combined source from peri-Gondwanan terranes and Laurentia to the north of the basin cannot be discredited.

Drainage area estimates for the Tullig sandstone IVF (TCL) from mean cross-set thickness yield a range (95% prediction interval) from ca. 1,140 km^2 to 99,000 km^2, with a base-case predicted value of ca. 10,600 km^2. Avalonia was of sufficient size to host a catchment of such limited extent. Drainage area estimates for the Kilkee sandstone IVF (KCL) yield a range (95% prediction interval) from ca. 46,000 km^2 to 4,108,000 km^2 with a most-likely predicted value of ca. 435,000 km^2. This reveals that the Kilkee sandstones of the Clare Basin must have been deposited by a river system with a continental-scale or at least regional-scale catchment. The relatively small terrane of Avalonia might have been too limited in size to host the entirety of this drainage basin, supporting the hypothesis of a combined source from both Avalonia and Laurentia. Palaeogeographic reconstructions (**Fig. 14D**) indicate that, during the late Kinderscoutian, a river network draining from Laurentia might have reached the Clare Basin and flowed into the basin eastward or southeastward, while drainage networks sourced from the south flowed northeastward into Clare Basin, as indicated by palaeocurrent data (Pulham, 1989). In the Clare Basin, these two catchments amalgamated into a single larger catchment, which potentially may have acted as a source to contemporaneous deep-water turbidites.

South Wales Basin

A speculative palaeogeographic model by George (2001) proposed that the late Yeadonian Farewell Rock IVF of South Wales (FRS) might represent a preserved part of the routing system for the late Namurian turbidites (Crackington Formation) of the Culm Basin. Other authors (Freshney et al., 1979; Melvin, 1986; Burne, 1995; Hartley, 1993) have demonstrated a northerly provenance for these turbidites on the basis of sedimentological data. However, based on channel orientation and palaeoflow analysis, Rippon (1996) inferred that the deposits of Westphalian A-B sedimentary strata of the Culm Basin and South Wales Basin were derived from a common, distant southerly source. This implies that combined northerly-southerly sources for the late Namurian turbidites of the Culm basin cannot be ruled out on the basis of the available data.

The estimated average value of mean bankfull depth for the formative rivers of the Farewell Rock incised valley is ca. 10 m, returning an estimated drainage area with a base-case value of ca. 50,000 km^2. Hence, this regional-scale river system, being derived from the emergent Wales-Brabant High, a localized high (George, 2001), could only provide limited supply of sediment to the late Namurian turbidites of the Culm basin. The hypothesis of an additional sediment source from the south appears therefore likely. However, mass-balance analysis of the sediment volume derivable from the source and deposited in the basin is necessary to substantiate this assumption.

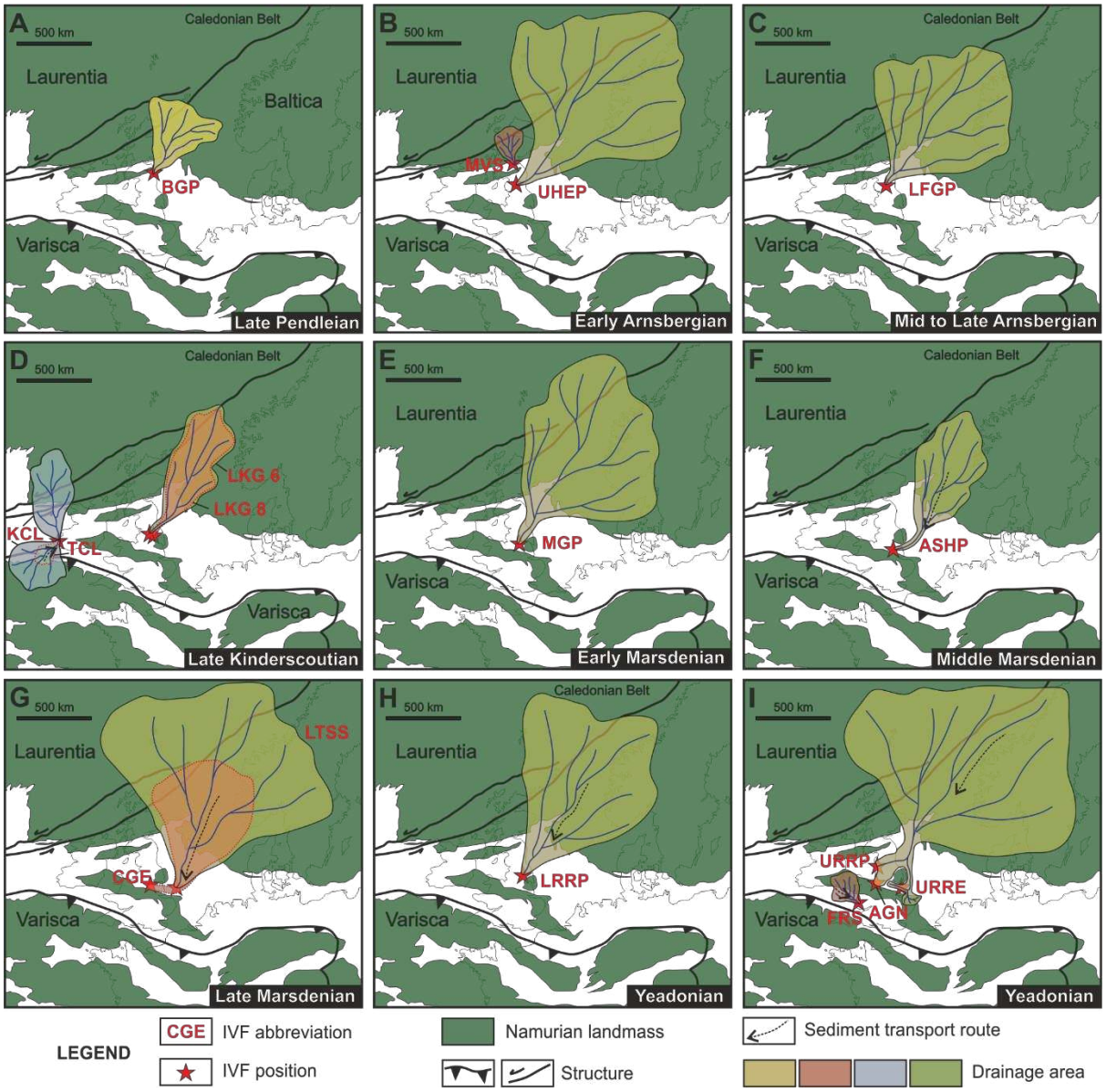

Fig. 14. Palaeogeographic reconstruction maps for basins in the UK and Ireland during Namurian time, presented by regional substage. Green outlines of palaeo-landmasses adapted from reconstructions of Blakey (2016). Black dashed arrows denote sediment transport paths inferred from existing provenance studies (detrital zircon age dating, heavy mineral analyses, petrographic data) and sedimentological data (palaeocurrent or palaeogradient indicators). Note that the size of drainage areas for each IVF used for regional palaeogeographic reconstructions represents either (i) the average of the base-case predicted value estimated from the average modern analogue and that estimated from IVF dimension, or (ii) the value obtained with either of these two methods if data on cross-set thickness or IVF dimension are lacking.

CONCLUSIONS

A database-driven synthesis of data from 18 Namurian incised-valley fills in the UK and Ireland has been performed to quantitatively estimate palaeohydrological characteristics of their formative river systems, and to attempt refinement of the regional palaeogeographic reconstructions of their basins. The main findings are summarized as follows.

(i) The facies architecture of fluvial deposits of the studied IVFs suggests that the palaeorivers feeding the Namurian IVFs of the UK and Ireland were likely

perennial and perhaps characterized by relatively limited variations in discharge. The notion of low discharge variability is in accord with inferences of a predominantly humid tropical climate prevailing in the study areas, located near the equator during the Namurian. However, the coefficient of variation of the thickness of sets of dune-scale cross-stratification for the studied deposits is characteristically low, and this might be a record of some celerity of flood recession driving bedform disequilibrium and high bedform preservation.

(ii) In four examples, inferences on river bathymetry based on limited observations of the thickness of bar and channel-fill elements return consistently smaller channel depths than estimations based on cross-set thickness statistics. In other four cases, projected values of maximum bankfull depths are larger than the decompacted thickness of the IVFs. Limitations in data and interpretations (e.g., misidentification of dune *versus* unit-bar cross-sets) and high bedform preservation linked to bedform disequilibrium are acknowledged as possible causes, but a conclusive explanation of these inconsistencies has not been reached.

(iii) Reconstruction of the size of IVF drainage areas has been attempted based on integration of flow-depth estimations from dune-scale cross-set thickness statistics with scaling relationships of IVF dimensions derived from late-Quaternary IVFs (Wang et al., 2019). This approach allowed effective consideration of a range of uncertainties in rock-record observations and in resulting extrapolations.

(iv) Relationships between estimated drainage areas and the relative proportions of facies that may have been deposited under lower- *versus* upper-flow-regime or transitional to upper-flow-regime conditions might reflect the fact that the size of drainage areas controls the facies architecture of fluvial deposits within incised valleys through its effect on variability in water discharge.

(v) The proposed estimations of the size of drainage areas provide complementary insight to existing provenance and sedimentological data, as they enable tentative reconstructions of source-to-sink systems in the context of the regional palaeogeographic configuration for the Namurian.

The approaches illustrated in this work can be replicated to the study of palaeohydrologic characteristics and palaeogeographic reconstructions of incised-valley fills globally and through geological time.

ACKNOWLEDGEMENTS

Ru Wang has been supported by a scholarship from China Scholarship Council associated with the University of Leeds (Grant number 201606440059). FRG-ERG and SMRG sponsors and partners AkerBP, Areva (now Orano), BHPBilliton, Cairn India (Vedanta), ConocoPhillips, Chevron, Debmarine, Engie, Equinor, Murphy Oil, Nexen-CNOOC, Occidental, Petrotechnical Data Systems, Saudi Aramco, Shell, Tullow Oil, Woodside and YPF are thanked for their financial support of the research. Ru Wang thanks the International Association of Sedimentologists for provision of a Postgraduate Research Grant that enabled field data collection for part of this study in Pembrokeshire, South Wales, UK. Soma Budai is thanked for fieldwork assistance. Roman Soltan is thanked for kindly offering several published papers on the geology of the Pennine Basin and giving advice on fieldwork. Xin Zhao is thanked for giving advice on statistical methods. Two anonymous reviewers and Associate Editor Piret Plink-Björklund are thanked for their constructive comments, which have substantially improved the article.

REFERENCES CITED

Alqahtani, F.A., **Johnson, H.D.**, **Jackson, C.A.L.** and **Som, M.R.B.** (2015) Nature, origin and evolution of a Late Pleistocene incised valley-fill, Sunda Shelf, Southeast Asia. *Sedimentology*, **62**, 1198-1232.

Allen, J.R.L. (1982) Sedimentary Structures: Their Character and Physical Basis. Elsevier, New York.

Anderson, J.B., **Rodriguez, A.**, **Abdulah, K.C.**, **Fillon, R.H.**, **Banfield, L.A.**, **McKeown, H.A.** and **Wellner, J.S.** (2004) Late Quaternary stratigraphic evolution of the northern Gulf of Mexico margin: a synthesis. In: *Late Quaternary Stratigraphic Evolution of the Northern Gulf of Mexico Margin: A Synthesis* (Eds J.B. Anderson and R.H. Fillon). *SEPM Spec. Publ.*, **79**, 1–23.

Bartholdy, J., **Ernstsen, V.B.**, **Flemming, B.W.**, **Winter, C.**, **Bartholomä, A.** and **Kroon, A.** (2015) On the formation of current ripples. *Sci. Rep.*, **5**, 11390.

Beighley, R.E. and **Gummadi, V.** (2011) Developing channel and floodplain dimensions with limited data: a case study in the Amazon Basin. *Earth Surf. Process. Landforms*, **36**, 1059–1071.

Best J., **Wignall P. B.**, **Stirling E. J.**, **Obrock E.** and **Bryk A.** (2006) The Tullig and Kilkee Cyclothems in Southern County Clare. In: *A Field Guide to the Carboniferous Sediments of the Shannon Basin, Western Ireland* (Eds J. L. Best and P. B. Wignall), *IAS Field Guide*, 240-328.

Bijkerk J. F. (2014) External controls on sedimentary sequences: a field and analogue modelling-based study. Unpublished PhD Thesis, University of Leeds, UK.

Blakey, R. (2016) Library of Paleogeography, Colorado Plateau Geosystems™, Arizona, USA. http://deeptimemaps.com/global-paleogeography-and-tectonics-in-deep-time-series/ (accessed 21 November 2019).

Blakey, R.C. and **Wong, T.E.** (2007) Carboniferous–Permian paleogeography of the assembly of Pangaea. In: *Proceedings of the XVth International Congress on Carboniferous and Permian Stratigraphy* (Ed T.E. Wong). Utrecht, 10-16 August 2003, pp. 443-456. Royal Netherlands Academy of Arts and Sciences, Amsterdam.

Blum, M.D. and **Womack, J.H.** (2009) Climate change, sea-level change, and fluvial sediment supply to deepwater systems. In: *External Controls on Deep Water Depositional Systems: Climate, Sea-Level, and Sediment Flux* (Eds B. Kneller, O.J. Martinsen and B. McCaffrey), *SEPM Spec. Publ.*, **92**, 15–39.

Blum, M., **Martin, J.**, **Milliken, K.** and **Garvin, M.** (2013) Paleovalley systems: insights from Quaternary analogs and experiments. *Earth-Sci. Rev.*, **116**, 128–169.

Boucot, A.J., **Xu, C.**, **Scotese, C.R.** and **Morley, R.J.** (2013) Phanerozoic paleoclimate: an atlas of lithologic indicators of climate. In: *SEPM Concepts in Sedimentology and Paleontology* (Eds G. J. Nichols and B. Ricketts), pp. 478. SEPM, Tulsa, Oklahoma.

Bowen, D.W. and **Weimer, P.** (2003) Regional sequence stratigraphic setting and reservoir geology of Morrow incised-valley sandstones (lower Pennsylvanian), eastern Colorado and western Kansas. *AAPG Bull.*, **87**, 781–815.

Boyd, R., **Dalrymple, R.W.** and **Zaitlin, B.A.** (2006) Estuarine and incised-valley facies model. In: *Facies Models Revisited* (Eds H.W. Posamentier and R.G. Walker). *SEPM Spec. Publ.*, **84**, 171–235.

Bradley, R. W. and **Venditti, J. G.** (2017) Reevaluating dune scaling relations. Earth-Sci. Rev., **165**, 356–376.

Brettle, M. J. (2001) Sedimentology and high-resolution sequence stratigraphy of shallow water delta systems in the early Marsdenian (Namurian) Pennine Basin, Northern England. Unpublished PhD Thesis, University of Liverpool, UK.

Brettle, M. J., **McIlroy, D.**, **Elliott, T.**, **Davies, S. J.** and **Waters, C. N.** (2002) Identifying cryptic tidal influences within deltaic successions: an example from the Marsdenian (Namurian) interval of the Pennine Basin, UK. *J. Geol. Soc.*, **159**, 379-391.

Bridge, J. S. (1997). Thickness of sets of cross strata and planar strata as a function of formative bed-wave geometry and migration, and aggradation rate. *Geology*, **25**, 971-974.

Bridge, J.S. and **Tye, R.S.** (2000) Interpreting the dimensions of ancient fluvial channel bars, channels, and channel belts from wireline-logs and cores. *AAPG Bull.*, **84**, 1205-1228.

Bridge, J.S. (2003) Rivers and Floodplains: Forms, Processes, and Sedimentary Record. John Wiley & Sons, Malden, Massachusetts, 491 pp.

Bridge, J.S. (2006) Fluvial facies models: recent developments. In: *Facies Models Revisited* (Eds H.W. Posamentier and R.G. Walker). *SEPM Spec. Publ.*, **84**, 85–170.

Bristow, C.S. (1988) Controls on the sedimentation of the Rough Rock Group (Namurian) from the Pennine Basin of northern England. In: *Sedimentation in a Synorogenic Basin Complex: The Upper Carboniferous of Northwest Europe* (Eds B.M. Besly and G. Kelling), pp. 114-131. Blackie, Glasgow.

Bristow, C.S. and **Myers, K.J.** (1989) Detailed sedimentology and gamma-ray log characteristics of a Namurian deltaic succession I: Sedimentology and facies analysis. In: *Deltas: Sites and Traps for Fossil Fuels* (Eds M. K. G. Whateley and K. T. Pickering). *Geol. Soc. London Spec. Publ.*, **41**, 75-80.

Bristow, C.S. (1993) Sedimentology of the Rough Rock: a Carboniferous braided river sheet sandstone in northern England. In: *Braided Rivers* (Eds J. L. Best and C. S. Bristow). *Geol. Soc. London Spec. Publ.*, **75**, 291-304.

Broadhurst, F. M., **Simpson, I. M.** and **Hardy, P. G.** (1980) Seasonal sedimentation in the Upper Carboniferous of England. *J. Geol.*, **88**, 639-651.

Buller, T., **Eriksson, K.A.** and **McClung, W.S.** (2018) Upstream controls on incised-valley dimensions and fill: Examples from the Upper Mississippian Mauch Chunk Group, Central Appalachian Basin, USA. *Palaeogeogr. Palaeoclimatol. Palaeoecol.*, **490**, 355-374.

Burne, R.V. (1995) The return of the fan that never was: Westphalian turbidite systems in the Variscan Culm Basin: Bude Formation (southwest England). In: *Sedimentary Facies Analysis* (Ed A.G. Plint). *IAS Spec. Publ.*, **22**, 101-135.

Chadwick, R.A., **Holliday, D.W.**, **Holloway, S.** and **Hulbert A.G.** (1995) The Structure and Evolution of the Northumberland-Solway Basin and Adjacent Areas. London, British Geological Survey Subsurface Memoir, Her Majesty's Stationery Office, 90 pp.

Chaloner, W. G. and **Creber, G. T.** (1990) Do fossil plants give a climatic signal? *J. Geol. Soc. London*, **147**, 343-350.

Church, K. D. and **Gawthorpe, R. L.** (1994) High resolution sequence stratigraphy of the late Namurian in the Widmerpool Gulf (East Midlands, UK). *Mar. Petrol. Geol.*, **11**, 528-544.

Collier, J.S., **Oggioni, F.**, **Gupta, S.**, **García-Moreno, D.**, **Trentesaux, A.** and **De Batist, M.** (2015) Streamlined islands and the English Channel megaflood hypothesis. *Global Planet. Change*, **135**, 190-206.

Collinson, J. D. (1988) Controls on Namurian sedimentation in the Central Province Basins of northern England. In: *Sedimentation in a Synorogenic Basin Complex: the Upper Carboniferous of Northwest Europe* (Eds B.M. Besly and G. Kelling), pp. 85-101. Blackie, Glasgow.

Collinson, J.D. (1996) Alluvial sediments. In: *Sedimentary Environments: Processes, Facies and Stratigraphy* (Ed H.G. Reading), pp. 37–82. Blackwell Science, Oxford.

Collinson, J.D., **Evans, D.J.**, **Holliday, D.W.** and **Jones, N.S.** (2005) Dinantian and Namurian depositional systems in the southern North Sea. In: *Carboniferous Hydrocarbon Geology: The Southern North Sea and Surrounding Onshore Basins* (Eds J.D. Collinson, D.J. Evans, D.W. Holliday and N.S. Jones). *Yorks. Geol. Soc. Spec. Publ.*, **7**, 35-56.

Collinson, J.D., **Martinsen, O.**, **Bakken, B.** and **Kloster, A.** (1991) Early fill of the western Irish Namurian Basin; a complex relationship between turbidites and deltas. **Basin Res.**, **3**, 223–242.

Colombera, L. and **Mountney, N.P.** (2019) The lithofacies organization of fluvial channel deposits: A meta-analysis of modern rivers. *Sed. Geol.*, **383**, 16-40.

Colombera, L., **Mountney, N.P.** and **McCaffrey, W.D.** (2012) A relational database for the digitization of fluvial architecture: concepts and example applications. *Petrol. Geosci.*, **18**, 129–140.

Colombera, L., **Mountney, N.P.** and **McCaffrey, W.D.** (2013) A quantitative approach to fluvial facies models: methods and example results. *Sedimentology*, **60**, 1526–1558.

Crowley, T.J. and **Baum, S.K.** (1991) Estimating Carboniferous sea-level fluctuations from Gondwanan ice extent. *Geology*, **19**, 975-977.

Davidson, S.K. and **North, C.P.** (2009) Geomorphological regional curves for prediction of drainage area and screening modern analogues for rivers in the rock record. *J. Sediment. Res.*, **79**, 773-792.

Davies, S.J. (2008) The record of Carboniferous sea-level change in low-latitude sedimentary successions from Britain and Ireland during the onset of the late Paleozoic ice age. In: *Resolving the Late Paleozoic Ice Age in Time and Space* (Eds C.R. Fielding, T.D. Frank and J.L. Isbell). *Geol. Soc. Am. Spec. Pap.*, **441**, 187–204.

Davies, S.J., **Hampson, G.J.**, **Elliott, T.** and **Flint, S.S.** (1999) Continental scale sequence stratigraphy of the Upper Carboniferous and its applications to reservoir prediction. In: *Petroleum Geology of Nortwest Europe* (Eds A. J. Fleet and S. A. R. Boldy). *Proceedings of the 5th Petroleum Geology Conference*: London, Geological Society of London, pp. 757–770.

Davis, J.C. (2002) Statistics and Data Analysis in Geology, 3rd ed. Wiley, New York.

Dean, M.T., **Browne, M.A.E.**, **Waters, C.N.** and **Powell, J.H.** (2011) A lithostratigraphical framework for the Carboniferous successions of northern Great Britain (onshore). *British Geological Survey Research Report*, RR/10/07.

Dunne, W.M., **Hancock, P.L.** and **Tringham, M.E.** (1980) The structure of SW Dyfed. *Proc. Geol. Assoc.*, **91**, 237-238.

Dunne, W.M. (1983) Tectonic evolution of SW Wales during the Upper Palaeozoic. *J. Geol. Soc. London*, **140**, 257-265.

Ellen, R., **Browne, M.A.E.**, **Mitten, A.J.**, **Clarke, S.M.**, **Leslie, A.G.** and **Callaghan, E.** (2019) Sedimentology, architecture and depositional setting of the fluvial Spireslack Sandstone of the Midland Valley, Scotland: insights from the Spireslack surface coal mine. In: *River to Reservoir: Geoscience to Engineering* (Eds P.W.M. Corbett, A. Owen, A.J. Hartley, S. Pla-Pueyo, D. Barreto, C. Hackney and S.J. Kape). *Geol. Soc. Spec Publ.*, **488**, SP488-2.

Falcon-Lang, H. J. (2000) Fire ecology of the Carboniferous tropical zone. *Palaeogeogr. Palaeoclimatol. Palaeoecol.*, **164**, 339-355.

Falcon-Lang, H. J. and **Scott, A. C.** (2000) Upland ecology of some Late Carboniferous cordaitalean trees from Nova Scotia and England. *Palaeogeogr. Palaeoclimatol. Palaeoecol.*, **156**, 225-242.

Fielding, C.R., **Alexander, J.** and **Allen, J.P.** (2018) The role of discharge variability in the formation and preservation of alluvial sediment bodies. *Sed. Geol.*, **365**, 1–20.

Fielding, C.R., **Allen, J.P.**, **Alexander, J.** and **Gibling, M.R.** (2009) Facies model for fluvial systems in the seasonal tropics and subtropics. *Geology*, **37**, 623–626.

Freshney, E.C., **Edmonds, E. A.**, **Taylor, R. T.** and **Williams, B. J.** (1979) Geology of the country around Bude and Bradworthy. *Geol. Surv. Great Brit. Mem.* HMSO, London.

Ganti, V., **Paola, C.** and **Foufoula-Georgiou, E.** (2013) Kinematic controls on the geometry of the preserved cross sets. *J. Geophys. Res. Earth Surf.*, **118**, 1296–1307.

Ganti, V., **Whittaker, A. C.**, **Lamb, M. P.** and **Fischer, W. W.** (2019a) Low-gradient, single- threaded rivers prior to greening of the continents. *Proc. Nat. Acad. Sci.*, **116**, 11652–11657.

Ganti, V., **Lamb, M. P.** and **Chadwick, A. J.** (2019b) Autogenic Erosional Surfaces in Fluvio- deltaic Stratigraphy from Floods, Avulsions, and Backwater Hydrodynamics. *J. Sediment. Res.*, **89**, 815–832.

Gawthorpe, R.L., **Gutteridge, P.** and **Leeder, M.R.** (1989) Late Devonian and Dinantian basin evolution in northern England and North Wales. In: *The Role of Tectonics in Devonian and Carboniferous Sedimentation in the British Isles* (Eds R.S. Arthurton, P. Gutteridge and C. Nolan), *Yorks. Geol. Soc. Spec. Publ.*, **6**, 1–23.

George G. T. (2001) Late Yeadonian (Upper Sandstone Group) incised valley supply and depositional systems in the South Wales peripheral foreland basin: implications for the evolution of the Culm Basin and for the Silesian hydrocarbon plays of onshore and offshore UK. *Mar. Petrol. Geol.*, **18**, 671-705.

Gibling, M.R. (2006) Width and thickness of fluvial channel bodies and valley fills in the geological record: A literature compilation and classification. *J. Sed. Res.*, **76**, 731–770.

Gibling, M.R., **Fielding, C.R.** and **Sinha, R.** (2011) Alluvial valleys and alluvial sequences: towards a geomorphic assessment. In: *From River to Rock Record: The Preservation of Fluvial Sediments and Their Subsequent Interpretation* (Eds S.K. Davidson, S. Leleu and C. North), *SEPM Spec. Publ.*, **97**, 423–447.

Hallsworth, C.R. and **Chisholm, J.I.** (2008) Provenance of late Carboniferous sandstones in the Pennine Basin (UK) from combined heavy mineral, garnet geochemistry and palaeocurrent studies. *Sed. Geol.*, **203**, 196-212.

Hallsworth, C.R., **Morton, A.C.**, **Claoué-Long, J.** and **Fanning, C.M.** (2000) Carboniferous sand provenance in the Pennine Basin, UK: constraints from heavy mineral and detrital zircon age data. *Sed. Geol.*, **137**, 147–185.

Hamblin, W.K. (1965) Internal structures of" homogeneous" sandstones. Bull. *Kansas State Geol. Surv.*, **175**, 569–582.

Hampson, G.J. (1995) Incised valley fills and sequence stratigraphy of selected carboniferous delta systems in the UK. Unpublished PhD Thesis, University of Liverpool.

Hampson, G.J. (1997) A sequence stratigraphic model for deposition of the Lower Kinderscout Delta, an Upper Carboniferous turbidite-fronted delta. *Proc. Yorkshire Geol. Soc.*, **51**, 273-296.

Hampson, G.J., **Elliott, T.** and **Flint, S.S.** (1996) Critical application of high resolution sequence stratigraphic concepts to the Rough Rock Group (Upper Carboniferous) of northern England. In: High resolution sequence stratigraphy: innovations and applications (Eds Howell, J. A. and Aitken, J. F.), *Geol. Soc. London Spec. Publ.*, **104**, 221-246.

Hampson, G.J., **Davies, S.J.**, **Elliott, T.**, **Flint, S.S.** and **Stollhofen, H.** (1999) Incised valley fill sandstone bodies in Upper Carboniferous fluvio–deltaic strata: recognition and reservoir characterization of Southern North Sea analogues. In: *Petroleum Geology of Northwest Europe: Proceedings of the 5th Conference* (Eds A.J. Fleet and S.A.R. Boldy), pp. 771-788. Geological Society of London.

Hancock, P.L. and **Tringham, M.E.** (1983) Variscan deformation in southwest Wales. In: *The Variscan foldbelt in the British Isles* (Ed P.L. Hancock), pp. 47-73. Adam Hilgler, Bristol.

Hansford, M.R., **Plink-Björklund, P.** and **Jones, E.R.** (2020) Global quantitative analyses of river discharge variability and hydrograph shape with respect to climate types. *Earth-Sci. Rev.*, 102977.

Hartley, A.J. (1993) Silesian sedimentation in south-west Britain: sedimentary responses to the developing Variscan Orogeny. In: *Rhenohercynian and Subvariscan Fold Belts* (Eds R. A. Gayer, R. O. Greiling and A. K. Voger), pp. 159-196. Braunschweig, Vieweg.

Holbrook, J.M. and **Bhattacharya, J.P.** (2012) Reappraisal of the sequence boundary in time and space: case and considerations for an SU (subaerial unconformity) that is not a sediment bypass surface, a time barrier, or an unconformity. *Earth-Sci. Rev.*, **113**, 271-302.

Holbrook, J. and **Wanas, H.** (2014) A fulcrum approach to assessing source-to-sink mass balance using channel paleohydrologic paramaters derivable from common fluvial data sets with an example from the Cretaceous of Egypt. *J. Sediment. Res.*, **84**, 349-372.

Holdsworth, B.K. and **Collinson, J.D.** (1988) Millstone Grit cyclicity revisited. In: *Sedimentation in a Synorogenic Basin Complex: The Upper Carboniferous of Northwest Europe* (Eds B.M. Besly and G. Kelling), pp. 132-152. Blackie, Glasgow.

IBM Corp. Released (2015) IBM SPSS Statistics for Windows, Version 23.0. Armonk, NY: IBM Corp.

Jackson, R.G. (1975) Hierarchical attributes and a unifying model of bed forms composed of cohesionless material and produced by shearing flow. *GSA Bull.*, **86**, 1523–1533.

James, G., **Witten, D.**, **Hastie, T.** and **Tibshirani, R.** (2013) An introduction to statistical learning. Springer, New York.

Jerolmack, D. J. and **Mohrig, D.** (2005) Frozen dynamics of migrating bedforms. *Geology*, **33**, 57–60.

Jerrett R. M. and **Hampson G. J.** (2007) Sequence stratigraphy of the upper Millstone Grit (Yeadonian, Namurian), North Wales. *Geol. J.*, **42**, 513-530.

Jones C. M. and **Chisholm J. I.** (1997) The Roaches and Ashover Grits: sequence stratigraphic interpretation of a 'turbidite-fronted delta' system. *Geol. J.*, **32**, 45-68.

Kane, I. and **Hodgson, D. M.** (2015) Supercritical-flow structures on a Late Carboniferous delta front: Sedimentologic and paleoclimatic significance: Comment. *Geology*, **43**, 374-374.

Kirby, G.A., **Baily, H.E.**, **Chadwick, R.A.**, **Evans, D.J.**, **Holliday, D.W.**, **Holloway, S.**, **Hulbert, A.G.**, **Pharaoh, T.C.**, **Smith, N.J.**, **Aitkenhead, N.** and **Birch, B.** (2000) The Structure and Evolution of the Craven Basin and Adjacent Areas. London, British Geological Survey Subsurface Memoir, Her Majesty's Stationery Office, 130 pp.

Leary, K. C. P. and **Ganti, V.** (2020). Preserved fluvial cross strata record bedform disequilibrium dynamics. *Geophys. Res. Lett.*, **47**, e2019GL085910. https://doi.org/10.1029/2019GL085910.

Leclair, S. F., **Bridge, J. S.** and **Wang, F.** (1997) Preservation of cross-strata due to migration of subaqueous dunes over aggrading and non-aggrading beds: Comparison of experimental data with theory. *Geosci. Can.*, **24**, 55–66.

Leclair, S. F. and **Bridge, J. S.** (2001) Quantitative Interpretation of Sedimentary Structures Formed by River Dunes. *J. Sediment. Res.*, **71**, 713–716.

Leclair, S. F. (2002) Preservation of cross-strata due to the migration of subaqueous dunes: an experimental investigation. *Sedimentology*, **49**, 1157–1180.

Liebmann B. and **Mechoso C. R.** (2011) The South American monsoon system. In: *The Global Monsoon System: Research and Forecast* (Eds C.P. Chang, Y. Ding, N.C. Lau, R.H. Johnson, B. Wang and T. Yasunari), pp. 137–157. World Scientific Publishing, New Jersey.

Martin, J., **Cantelli, A.**, **Paola, C.**, **Blum, M.** and **Wolinsky, M.** (2011) Quantitative modeling of the evolution and geometry of incised valleys. *J. Sediment. Res.*, **81**, 64–79.

Martinsen O. J. (1990) Interaction Between Eustacy, Tectonics and Sedimentation with Particular Reference to the Namurian E1c-H2c of the Craven-Askrigg Area, Northern England. Unpublished PhD Thesis, Universitetet i Bergen, Norway.

Materia, S., **Gualdi, S.**, **Navarra, A.** and **Terray, L.** (2012) The effect of Congo River freshwater discharge on Eastern Equatorial Atlantic climate variability. *Clim. Dyn.*, **39**, 2109-2125.

Martinsen O. J. (1993) Depositional systems of the Craven-Askrigg Area, northern England: implications for sequence-stratigraphic models. In: *Sequence Stratigraphy and Facies Associations* (Eds H. W. Posamentier, C. P. Summerhayes, B. U. Haq and G. P. Allen), *IAS Spec. Publ.*, **18**, 247-281.

Martinsen O. J., **Collinson J. D.** and **Holdsworth B. K.** (1995) Millstone Grit cyclicity revisited, II: sequence stratigraphy and sedimentary responses to changes of relative sea-level. In: *Sedimentary Facies Analysis* (Ed A. G. Plint). A Tribute to the Research and Teaching of Harold G. Reading. *IAS SPec. Publ.*, **22**, 305-327.

Maselli, V., **Trincardi, F.**, **Asioli, A.**, **Ceregato, A.**, **Rizzetto, F.** and **Taviani, M.** (2014) Delta growth and river valleys: the influence of climate and sea level changes on the South Adriatic shelf (Mediterranean Sea). *Quat. Sci. Rev.*, **99**, 146–163.

Mattheus, C.R. and **Rodriguez, A.B.** (2011) Controls on late Quaternary incised-valley dimension along passive margins evaluated using empirical data. *Sedimentology*, **58**, 1113–1137.

Mattheus, C.R., **Rodriguez, A.B.**, **Greene, D.L.**, **Simms, A.R.** and **Anderson, J.B.** (2007) Control of upstream variables on incised-valley dimension. *J. Sed. Res.*, **77**, 213–224.

Maynard, J.R. (1992) Sequence stratigraphy of the upper Yeadonian of northern England. *Mar. Petrol. Geol.*, **9**,197-207.

Maynard, J.R. and **Leeder, M.R.** (1992) On the periodicity and magnitude of Late Carboniferous glacio-eustatie sea-level changes. *J. Geol. Soc. London*, **149**, 303-311.

McCandless, T.L. (2003) Maryland Stream Survey: Bankfull Discharge and Channel Characteristics of Streams in the Coastal Plain Hydrologic Region. U.S. Fish and Wildlife Service, Report CBFO-S03-02.

Melvin, J. (1986) Upper Carboniferous fine-grained turbiditic sandstones from Southwest England; a model for growth in an ancient, delta-fed subsea fan. *J. Sediment. Res.*, **56**, 19-34.

Metcalf, C. (2004) Regional channel characteristics for maintaining natural fluvial geomorphology in Florida streams. U.S. Fish and Wildlife Service, Panama City Fisheries Resource Office.

Metcalf, C. and **Shaneyfelt, R.** (2005) Alabama Riparian Reference Reach and Regional Curve Study. U.S. Fish and Wildlife Service, Panama City Fisheries Resource Office.

Miall, A.D. (1996) The Geology of Fluvial Deposits: Sedimentary Facies, Basin Analysis, and Petroleum Geology. Springer-Verlag, Heidelberg.

Mitchum Jr, R.M. and **Van Wagoner, J.C.** (1991) High-frequency sequences and their stacking patterns: sequence-stratigraphic evidence of high-frequency eustatic cycles. *Sed. Geol.*, **70**, 131-160.

Myrow, P. M., **Jerolmack, D. J.** and **Perron, J. T.** (2018) Bedform Disequilibrium. *J. Sediment. Res.*, **88**, 1096–1113.

Nicholas, A. P., **Smith, G. H. S.**, **Amsler, M. L.**, **Ashworth, P. J.**, **Best, J. L.**, **Hardy, R. J.**, et al., 2016. The role of discharge variability in determining alluvial stratigraphy. *Geology*, **44**, 3–6.

O'Beirne A.M. (1996) Controls on Silesian sedimentation in the Pennine Basin, UK and Appalachian Basin, Eastern Kentucky. Unpublished PhD Thesis, Oxford Brookes University, UK.

O'Mara P. T., **Merryweather M.**, **Stockwel, M.** and **Bowler M. M.** (1999) The Trent Gas Field: correlation and reservoir quality within a complex Carboniferous stratigraphy. In: *Petroleum Geology of Nortwest Europe* (Eds A. J. Fleet and S. A. R. Boldy). *Proceedings of the 5th Petroleum Geology Conference*, London, Geological Society of London, pp. 809-821.

Parrish, J. T. (1993) Climate of the supercontinent Pangea. *J. Geol.*, **101**, 215-233.

Paola, C. and **Borgman, L.** (1991) Reconstructing random topography from preserved stratification. *Sedimentology*, **38**, 553–565.

Phillips, J.D. (2011) Drainage area and incised valley fills in Texas rivers: A potential explanation. *Sed. Geol.*, **242**, 65–70.

Plink-Björklund, P. (2015) Morphodynamics of rivers strongly affected by monsoon precipitation: review of depositional style and forcing factors. *Sed. Geol.*, **323**, 110–147.

Pointon, M.A., **Cliff, R.A.** and **Chew, D.M.** (2012) The provenance of Western Irish Namurian Basin sedimentary strata inferred using detrital zircon U–Pb LA-ICP-MS geochronology. *Geol. J.*, **47**, 77-98.

Posamentier, H.W. (2001) Lowstand alluvial bypass systems: incised vs. unincised. *AAPG Bull.*, **85**, 1771–1793.

Posamentier, H.W. and **Allen, G.P.** (1999) Siliciclastic Sequence Stratigraphy: Concepts and Applications. SEPM (Society for Sedimentary Geology), Tulsa, Oklahoma, 210 pp.

Powell, C.M. (1987) Inversion tectonics in SW Dyfed. *Proc. Geol. Assoc.*, **98**, 193-203.

Powell, C.M. (1989) Structural controls on Palaeozoic basin evolution and inversion in southwest Wales. *J. Geol. Soc. London*, **146**, 439-446.

Pulham, A. J. (1988) Depositional and syn-sedimentary deformation processes in Namurian deltaic sequences of West County Clare, Ireland. Unpublished PhD Thesis, University College of Swansea, UK.

Pulham, A.J. (1989) Controls on internal structure and architecture of sandstone bodies within Upper Carboniferous fluvial-dominated deltas, County Clare, western Ireland, In: *Deltas: Sites and Traps for Fossil Fuels* (Eds M.K.G. Whateley and K.T. Pickering), *Geol. Soc. London Spec. Publ.*, **41**, 179-203.

Reesink, A. J. H. (2019) Interpretation of cross strata formed by unit bars. In: *Fluvial Meanders and Their Sedimentary Products in the Rock Record* (Eds M. Ghinassi, L. Colombera, N.P. Mountney and A.J.H. Reesink), *IAS Spec. Publ.*, **48**, 173-200.

Riley, N.J., **Claoué-Long, J.C.**, **Higgins, A.C.**, **Owens, B.**, **Spears, A.**, **Taylor, L.** and **Varker, W.J.** (1995) Geochronometry and geochemistry of the European mid-Carboniferous boundary global stratotype proposal, Stonehead Beck, North Yorkshire, UK. *Ann. Soc Géol. Belg.*, **116**, 275–289.

Rippon, J.H. (1996) Sand body orientation, palaeoslope analysis and basin-fill implications in the Westphalian A–C of Great Britain. *J. Geol. Soc. London*, **153**, 881-900.

Rowley, D. B., **Raymond, A.**, **Parrish, J. T.**, **Lottes, A. L.**, **Scotese, C. R.** and **Ziegler, A. M.** (1985) Carboniferous paleogeographic, phytogeographic, and paleoclimatic reconstructions. *Int. J. Coal Geol.*, **5**, 7-42.

Rygel, M.C., **Fielding, C.R.**, **Frank, T.D.** and **Birgenheier, L.P.** (2008) The magnitude of Late Paleozoic glacioeustatic fluctuations: a synthesis. *J. Sediment. Res.*, **78**, 500-511.

Salem, A.M., **Ketzer, J.M.**, **Morad, S.**, **Rizk, R.R.** and **Al-Aasm, I.S.** (2005) Diagenesis and reservoir-quality evolution of incised-valley sandstones: evidence from the Abu Madi gas reservoirs (Upper Miocene), the Nile Delta basin, Egypt. *J. Sediment. Res.*, **75**, 572–584.

Schneider, C.A., **Rasband, W.S.** and **Eliceiri, K.W.** (2012) NIH Image to ImageJ: 25 years of image analysis. *Nat. Methods*, **9**, 671.

Scotese, C.R. and **McKerrow, W.S.** (1990) Revised world maps and introduction. In: McKerrow, W.S., Scotese, C.R. (Eds.), Palaeozoic Palaeogeography and Biogeography. *Geol. Soc. London Mem.*, **12**, 1–21.

Simms, A.R., **Aryal, N.**, **Miller, L.** and **Yokoyama, Y.** (2010) The incised valley of Baffin Bay, Texas: a tale of two climates. *Sedimentology*, **57**, 642–669.

Smallwood, S.S. (1985) A thin-skinned thrust model for Variscan Pembrokeshire, Wales. *J. Struct. Geol.*, **7**, 683-687.

Soltan, R. and **Mountney, N.P.** (2016) Interpreting complex fluvial channel and barform architecture: Carboniferous Central Pennine Province, northern England. *Sedimentology*, **63**, 207-252.

Sømme, T.O., **Helland-Hansen, W.**, **Martinsen, O.J.** and **Thurmond, J.B.** (2009) Relationships between morphological and sedimentological parameters in source-to-sink systems: A basis for predicting semi-quantitative characteristics in subsurface systems. *Basin Res.*, **21**, 361–387.

Stephen, K.D. and **Dalrymple, M.** (2002) Reservoir simulations developed from an outcrop of incised valley fill strata. *AAPG Bull.*, **86**, 797–822.

Stirling E. J. (2003) Architecture of fluvio-deltaic sandbodies: the Namurian of Co. Clare, Ireland, as an analogue for the Plio-Pleistocene of the Nile Delta. Unpublished PhD Thesis, University of Leeds, UK.

Strong, N. and **Paola, C.** (2006) Fluvial landscapes and stratigraphy in a flume. *Sed. Rec.*, **4**, 4–8.

Strong, N. and **Paola, C.** (2008) Valleys that never were: time surfaces versus stratigraphic surfaces. *J. Sed. Res.*, **78**, 579–593.

Sweet, W.V. and **Geratz, J.W.** (2003) Bankfull hydraulic geometry relationships and recurrence intervals for North Carolina's Coastal Plain. *American Water Resources Association Journal*, **39**, 861–871.

Syvitski, J.P.M., **Peckham, S.D.**, **Hilberman, R.** and **Mulder, T.** (2003) Predicting the terrestrial flux of sediment to the global ocean: a planetary perspective. *Sediment. Geol.*, **162**, 5–24.

Syvitski, J. P., **Cohen, S.**, **Kettner, A. J.** and **Brakenridge, G. R.** (2014) How important and different are tropical rivers?—An overview. *Geomorphology*, **227**, 5-17.

Talling, P.J. (1998) How and where do incised valleys form if sea level remains above the shelf edge? *Geology*, **26**, 87–90.

Trower, E. J., **Ganti, V.**, **Fischer, W. W.** and **Lamb, M. P.** (2018) Erosional surfaces in the Upper Cretaceous Castlegate Sandstone (Utah, USA): Sequence boundaries or autogenic scour from backwater hydrodynamics? *Geology*, **46**, 707–710.

USDA-NRCS-NWMC (2009) Regional hydraulic geometry curves. U.S. Department of Agriculture, Little Rock, AK, U.S.A (website: https://www.nrcs.usda.gov/wps/portal/nrcs/detail/national/water/manage/hydrology/?cid=nrcs143_015052 (accessed 1 March 2020)).

Van der Zwan, C. J., **Boulter, M. C.** and **Hubbard, R. N. L. B.** (1985) Climatic change during the Lower Carboniferous in Euramerica, based on multivariate statistical analysis of palynological data. *Palaeogeogr. Palaeoclimatol. Palaeoecol.*, **52**, 1-20.

Van Hinsbergen, D. J., **de Groot, L. V.**, **van Schaik, S. J.**, **Spakman, W.**, **Bijl, P. K.**, **Sluijs, A.** and **Brinkhuis, H.** (2015). A paleolatitude calculator for paleoclimate studies (model version 2.1). PloS one, **10**.

Ventra, D., **Cartigny, M. J.**, **Bijkerk, J. F.** and **Açikalin, S.** (2015) Forum Reply on: Supercritical-flow structures on a Late Carboniferous delta front: Sedimentologic and paleoclimatic significance. *Geology*, **43**, e375.

Ventra, D., **Cartigny, M. J.**, **Bijkerk, J. F.** and **Acikalin, S.** (2015) Supercritical-flow structures on a Late Carboniferous delta front: Sedimentologic and paleoclimatic significance. *Geology*, **43**, 731-734.

Walker, R.G. (1976) Facies Models 3. Sandy fluvial systems. *Geosci. Can.*, **3**, 101–109.

Wang, R., **Colombera, L.** and **Mountney, N.P.** (2019) Geologic controls on the geometry of incised-valley fills: Insights from a global dataset of late-Quaternary examples. *Sedimentology*, **66**, 2134-2168.

Wang, R., **Colombera, L.** and **Mountney, N.P.** (2020) Database-Driven Quantitative Analysis of the Stratigraphic Architecture of Incised-Valley Fills. *Earth-Sci. Rev.*, **102988**, 1-25.

Waters, C.N. and **Davies, S.J.** (2006) Carboniferous: extensional basins, advancing deltas and coal swamps. In: *The geology of England and Wales* (Eds P.J. Brenchley and P.F. Rawson), pp.173-223. Geological Society of London, London.

Waters C.N., **Chisholm J.I.**, **Benfield A.C.** and **O'Beirne A.M.** (2008) Regional evolution of a fluviodeltaic cyclic succession in the Marsdenian (late Namurian Stage, Pennsylvanian) of the Central Pennine Basin, UK. *Proc. Yorkshire Geol. Soc.*, **57**, 1-28.

Waters, C.N., **Waters, R.A.**, **Barclay, W.J.** and **Davies, J.R.** (2009) A lithostratigraphical framework for the Carboniferous successions of southern Great Britain (Onshore). British Geological Survey Research Report, RR/09/01.

Waters, C.N. and **Condon, D.J.** (2012) Nature and timing of Late Mississippian to Mid-Pennsylvanian glacio-eustatic sea-level changes of the Pennine Basin, UK. *J. Geol. Soc. London*, **169**, 37-51.

Wellner, R.W. and **Bartek, L.R.** (2003) The effect of sea level, climate, and shelf physiography on the development of incised-valley complexes: a modern example from the East China Sea. *J. Sed. Res.*, **73**, 926–940.

Wignall, P.B. and **Best, J.L.** (2000) The Western Irish Namurian Basin reassessed. *Basin Res.*, **12**, 59–78.

Witzke, B. J. (1990) Palaeoclimatic constraints for Palaeozoic palaeolatitudes of Laurentia and Euramerica. *Geol. Soc. London Mem.*, **12**, 57-73.

Wong, H.K., **Lüdmann, T.**, **Haft, C.**, **Paulsen, A. M.**, **Hübscher, C.** and **Geng, J.** (2003) Quaternary sedimentation in the Molengraaff paleo-delta, northern Sunda Shelf (southern South China Sea). In: *Tropical Deltas of Southeast Asia Pacific Region—Sedimentology, Stratigraphy, and Petroleum Geology* (Eds F.H. Sidi, D. Nummedal, P. Imbert, H. Darman and H.W. Posamentier), *SEPM Spec. Publ.*, **76**, 201–216.

Wright, V.P. and **Vanstone, S.D.** (2001) Onset of Late Palaeozoic glacio-eustasy and the evolving climates of low latitude areas: a synthesis of current understanding. *J. Geol. Soc. London*, **158**, 579-582.

Zaitlin, B.A., **Dalrymple, R.W.** and **Boyd, R.** (1994) The stratigraphic organization of incised-valley systems associated with relative sea-level change. In: *Incised-Valley Systems: Origin and Sedimentary Sequences* (Eds R.W. Dalrymple, R. Boyd and B.A. Zaitlin), *SEPM Spec. Publ.*, **51**, 45–60.